Response to the comments of referee #1

Comment:
This paper focuses on evaluating various pathways for conversion of SO2 to PM2.5 sulfate over the North China Plane, a topic that has generated a large number of published papers in the last 2 years or so. The modeling work here is likely the most comprehensive analysis comparing all current mechanisms. Whether the results are accurate or not is hard to assess, but this work does provide valuable new insights by contrasting all the possible (main) mechanisms. The paper is appropriate for publication in this journal; however, it could be improved by careful editing focusing on grammar and clearer explanations. Additional broad and specific comments are provided below.

We thank the reviewer for the helpful comments. The referee's comments are first given in black type, followed by our response to each in turn in blue type. Any changes to the manuscript in response to the comments are then given in quotation marks in red type.

Broad Comments:

1 It would be worthwhile stating somewhere (maybe include in Table 1) what fraction of the $PM_{2.5}$ mass is sulfate; ie, how important is this problem.
We added the mass concentration on different pollution level in Table 1. During haze periods in winter and summer field campaigns mentioned in the MS, the contribution of SO_4^{2-} mass to $PM_{2.5}$ dry mass is in the range of 4%-59%, with an average value as 15% in winter and in the range of 1%-52%, with an average value as 19% in summer. In the introduction part, we have cited the literatures to illustrate the importance of secondary sulfate during haze periods, thus we added the fractions data in Table 1 in the revised MS.

Table 1. Averaged results of observed meteorological parameters, trace gases concentrations transition metal concentrations such as Fe, Cu, Mn and calculated ALWC, ionic strength, pH and sulfate formation rates in different pollution conditions in two field campaigns (±1σ).

Parameters	Clean	Slightly polluted	Polluted	Highly polluted
		Winter		
…				
$PM_{2.5}$ (μg/m^3)	18.3±10.1	52.0±10.0	101.7±18.2	190.0±30.0
…				

	Summer			
…				
$PM_{2.5}$ (μg/m^3)	20.1±10.2	54.9±11.7	104.8±20.5	194.6±32.9
…				

The concentrations of Mn were estimated based on the ratio of Fe/Mn observed in urban Beijing in the literatures (summarized in **Table S9**). All mentioned aerosol data is particle matters diameter smaller than 2.5 μm and $PM_{2.5}$ refers to the dry mass concentration of fine particulate matters.

2 These authors find that the most important route involves transition metal ions, however the concentration of these species seems to be very uncertain since in this work only the total (elemental) concentration was measured and the actual TMI species concentrations had to be estimated based on estimated solubilities (which can vary over a large range). This substantial uncertainty needs to be addressed. For example, maybe the authors should provide a range in predicted sulfate formation rates for the TMI route, include this in the plots (say something similar to Fig 2, if possible) and discuss the implications (does it change the findings).

We added the following discussion of transition metal sensitivity on sulfate formation in PKU-17 winter field campaign in the revised SI Text S4, Figure S9 and Table S10.

Water soluble fraction of Fe, Mn and Cu can vary over a large range. A large part of the soluble metals is in the form of soluble organic complexes or hydroxides rather than ions in aerosol particles. There are evidences that the existence of various aerosol water soluble organic acids (oxalate, malonate, tartrate and humid acid) cause an enhancement of Fe, Cu and Mn solubility and the formation of metal-organic complex (Paris and Desboeufs, 2013; Wozniak et al., 2015; Tapparo et al., 2020). What's more, the dissolution of Fe and Mn is highly influenced by aerosol pH. Circumneutral pH leads to a supersaturated soluble Fe (III), which then precipitates out of the solution. For these reasons, the promotion of metal solubility may have non-proportional influences on the aqueous concentration TMI. We conducted the sensitivity analysis for the solubility of Fe from 1% to 15% (Scenario one with fixed aqueous Mn and Cu concentration consist with the base run in the MS, Scenario two with fixed ratio of soluble Fe/Mn and Fe/Cu mass, ie, Mn solubility in the range of 10% to 100%, Cu in 5% to 75%, as shown in Table S10). Other aerosol component concentration, ionic strength, ALWC, observed meteorological parameters and trace gases concentrations stay consistent with the base run.

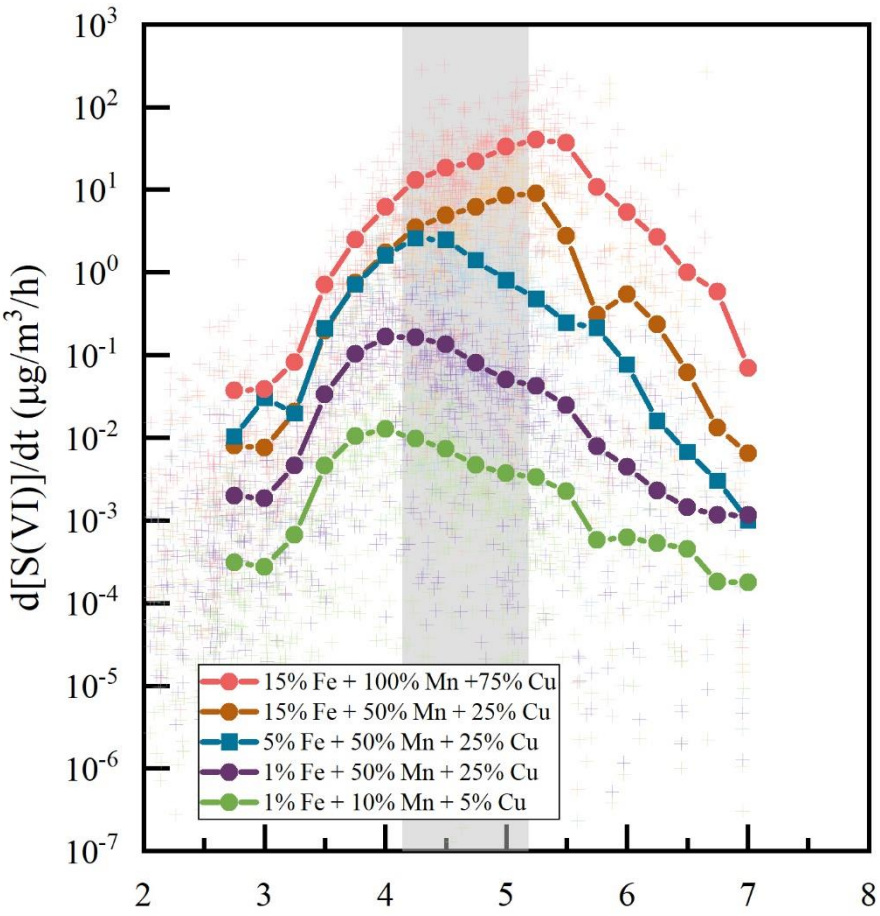

Figure S.9 Sensitivity analysis of transition metal including Fe, Mn and Cu solubility influences on the averaged sulfate formation rates in PKU-17 field observation. Dotted lines in the figure show the cluster averaged results with a pH span of 0.5 under actual ambient conditions with different transition metal solubilities.

Table S10. Base run and scenarios of the solubility sensitivity analysis.

Sensitivity Analysis	Solubility of transition metals	Sulfate formation contribution in haze pH range (4.2-5.2) (μg/m^3/h)
Base Run	5% Fe + 50% Mn + 25% Cu	0.80 - 2.58
Scenario 1	15% Fe + 50% Mn + 25% Cu	3.49 - 8.57
	1% Fe + 50% Mn + 25% Cu	0.05 - 0.16
Scenario 2	15% Fe + 100% Mn + 75% Cu	12.97 - 32.87
	1% Fe + 10% Mn + 5% Cu	0.009 - 0.004

As shown in Figure S.9, In the range of winter haze periods pH (4.2-5.2), averaged sulfate formation rates in PKU-17 field observation is non-proportional to the initial transition metal solubility. Fe solubility increasing from 1% to 5% will cause d[S(VI)]/dt to increase over an order of magnitude, and increasing to 15% cause no obvious effect when pH smaller than 4.2, while obvious effect the pH ranging from 4.2 to 6. This phenomenon may be due to the piecewise calculation equations of TMI-catalysis oxidizing SO_2 as mentioned in the SI and following. In the presence of TMI

organic complexes and redox reactions, this equation may need to be further verified, but verification is not within the scope of this study. It is obvious that the d[S(VI)]/dt changes caused by the proportional expansion of the solubility of the three transition metals (Scenario 2) is more significant especially when the solubility is reduced to 1%+10%+5%. Increasing of solubility to 15%Fe+100%Mn+75%Cu can increase sulfate formation rate to 5-84 times higher than in base run during haze periods pH as 4.2-5.2. This can explain to a certain extent that excessive TMI concentrations will not cause a sharp increase in d[S(VI)]/dt, which may be due to the buffering effect caused by the formation of organic complexes.

Part of Table S2. Aqueous-phase reaction rate expressions, rate constants (k) and influence of ionic strength (Is) on k for sulfate production in aerosol particle condensed phase.

Oxidants	The reaction rate expressions ($R_{S(IV)+oxi}$), constants (k) and influence of I_s (in unit of M) on k [a]	Notes	References
TMI+O_2 [f]	$k_6[H^+]^{-0.74}[S(IV)][Mn(II)][Fe(III)]$ (pH ≤ 4.2) $k_6 = 3.72\times10^7\times e^{(-8431.6\times(1/T-1/297))}$ M^{-2} s^{-1} $k_7[H^+]^{0.67}[S(IV)][Mn(II)][Fe(III)]$ (pH > 4.2) $k_7 = 2.51\times10^{13}\times e^{(-8431.6\times(1/T-1/297))}$ M^{-2} s^{-1}		Ibusuki and Takeuchi (1987)
	$\log_{10}(\frac{k}{k_{I_S=0}}) = \frac{b_4\sqrt{I_S}}{1+\sqrt{I_S}}$ [g] b_4 is in range of –4 to –2	$I_{s,\ max}$ = 2 M	Martin and Hill (1987, 1967)

3 The concentration of the TMIs (mainly Fe(II)+Fe(III)) and Mn involved in the surface reaction chemistry determines how fast sulfate is formed (line 97 notes that the TMI concentration is crucial…). But what are the TMI concentrations, only total metals measured by XRF are given? What is unique about these regions that makes these metal ions a major route? The authors point to the haze reducing photochemistry (during pollution events the PM2.5 mass is very high compared to many other regions globally), high RH, moderate particle pH, but what about the concentration of TMI? My rough analysis suggests that the mass ratio of TMI to sulfate is much higher in this region than many others, which would also be an important reason why this route may be important in this specific region. It would also support the conclusions of the paper, that emissions of these metals should be reduced (although as I note below, I believe more details are needed on the sources of the TMI, I don't think it is solely coal combustion based on the cited paper). I think the authors should assess this question; are TMI a uniquely large fraction of the PM2.5 or (TMI/sulfate ratio) in this region? At the very least, please provide some form of assessment of TMI mass concentrations, (this could include for example the sum of the various forms since the speciation is highly variable, eg,

Fe(II)+Fe(II), etc), relative to PM2.5 or sulfate, ie, maybe in Table 1.

In our calculation, aerosol pH, aerosol water content and high transition metal concentrations synthetically cause the aqTMI catalysis oxidation pathway an important contributor to secondary sulfate formation in PKU-17 winter field campaign in Beijing. The mass ratio of Fe total mass to SO_4^{2-} was in a high range compared to other observations in other regions, as shown in Table R1. However, the high concentration of transition metal does not mean that aqTMI play a role in sulfate formation. Proper aerosol liquid water content and aerosol pH ranging from 4 to 5.5 were the other two important factors improving the contribution percentage of aqTMI pathway. Compared to the total mass concentration of transition metal, effective aqueous TMI concentration is more relative to the sulfate formation. As shown in Figure 1 (c) and (d) in the MS, obvious correlations between αFe (III) (defined as the product of the Fe (III) activity coefficient, concentration, molecular weight (56) and aerosol liquid water content) and sulfate concentration were observed in the haze periods both in summer (R^2=0.63) and winter (R^2=0.71) and the correlation is consistent with verified the important contributions from aqTMI pathway to the sulfate formation. However, the calculation of αFe still has a large uncertainty (as discussed in the above response), so we can only compare the total Fe mass concentration and the sulfate concentration in various regions here in order to illustrate the high level of transition metal in Beijing.

The sources of transition metals including Fe, Mn and Cu is discussed in following response to comment 9.

Table R1. Fe/SO_4^{2-} ratio in different regions.

Location	Time	SO_4^{2-}	Fe	Fe/SO_4^{2-}	reference
PKU-17_highly polluted	2017	16.6 ± 6.6	1.30 ± 0.30	78.35	This study
PKU-17_polluted		8.3 ± 4.2	0.73 ± 0.26	87.35	
Hongkong	2001	12.76 ± 5.45	0.25 ± 0.12	19.59	(Ho et al., 2003)
		15.29 ± 3.71	0.48 ± 0.50	31.39	
		13.07 ± 5.17	0.19 ± 0.19	14.54	
Lanzhou	2014	12.0 ± 4.6	1.93 ± 0.95	161.08	(Wang et al., 2016b)
		7.6 ± 3.3	2.49 ± 1.55	327.24	
Fujian	2007	20.38 ± 5.85	0.58 ± 0.32	28.56	(Yin et al., 2012)
Guangzhou	2013	12.6 ± 7.6	0.16 ± 0.11	12.94	(Lai et al., 2016)
Suzhou	2014	17.3 ± 8.61	2.12 ± 2.73	122.54	(Liu et al., 2016)
		16.64 ± 8.61	0.96 ± 0.37	57.69	
		14.87 ± 9.27	0.73 ± 0.22	49.09	
Nanjing	2013	52.3 ± 35.7	0.98 ± 0.35	18.72	(Li et al., 2016)
		41.4 ± 27.2	1.10 ± 0.39	26.57	
Shanghai	2014	19.5 ± 9.98	1.85	94.87	(Ming et al., 2017)
		16.5 ± 7.7	1.89 ± 0.72	114.73	
Henan	2018	22.5 ± 10.1	4.14 ± 1.57	183.91	(Dong et

		3.2 ± 1.5	0.79 ± 0.32	246.53	al., 2020)
Los Angeles	2005-2018		0.19		(Farahani et al., 2021)
			0.014		
Thailand	2019	8.02 ± 1.96	0.64 ± 0.09	79.80	(Kayee et al., 2020)
Kaohsiung Harbor in Philippines	2019	6.8 ± 1.53	0.53 ± 0.08	77.94	(Tseng et al., 2021)
Manila Harbor in Taiwan		16.6 ± 6.6	1.30 ± 0.29	78.35	

4 Finally, throughout the paper it should be clarified that all particle concentrations reported are PM2.5.

We added the sentences in the Introduction part to clarified that all particle concentrations reported are $PM_{2.5}$ including total mass concentration of transition metals, water soluble ions and so on. And the mass concentration of $PM_{2.5}$ reported in the revised MS does not including particle water.

"…concentrations and the aerosol liquid water content (ALWC) on the aqueous reactant levels and the sulfate formation rate. All particle concentrations reported are fine particle matters with diameter below 2.5 μm ($PM_{2.5}$)."

Specific Comments

5 Abstract line 11, change hindes to hinders.

We change the word "hindes" to "hinders" in the revised MS abstract as "Lacking of detailed and comprehensive field data hinders the accurate evaluation of relative roles of prevailing sulfate formation pathways."

6 Line 83, can you provide plots of Fe and Mn vs PM2.5 mass? This would also help address one of the major points raised above?

We changed the Figure S4 in the revised SI. Total Mn mass concentration were estimated at the ratio of Fe/Mn equals to 28, thus the trend of Mn mass concentration was omitted in the figure.

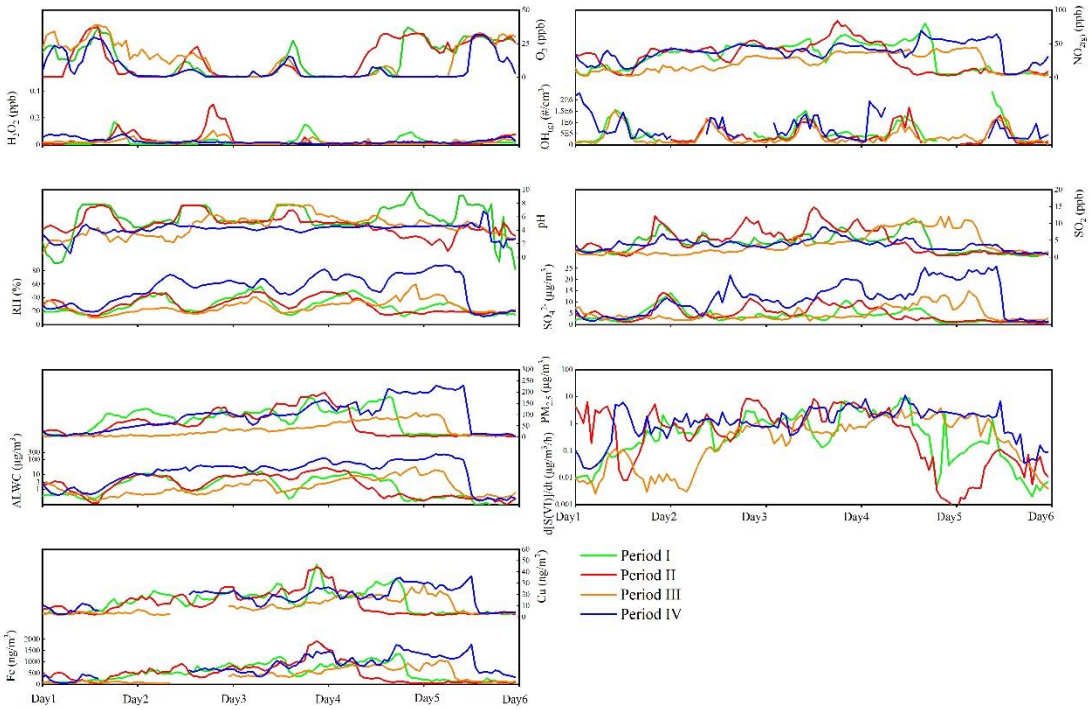

Fig. S4. Time series of observed gas-phase pollutants concentrations, RH, Temperature, $PM_{2.5}$ mass loading, Fe as well as Cu total mass concentrations and calculated aerosol pH and water content and sulfate formation rates in these four haze periods in PKU-17 field campaign.

7 Table 1 Description (above the table) is incomplete. There are also aerosol particle metal species data but not noted, etc. Is the aerosol data PM2.5, please specify?
8 Table 1. Why not add the PM2.5 mass ranges for each pollution level to the table? Or put in the Table caption.
We added the aerosol particle metal species data notes in the title of Table and clarified the meaning of reported aerosol data in the title and notes of Table 1 in the revised MS. We also added the data of $PM_{2.5}$ dry mass concentration in Table 1. Please see the response above.

9 Lines 99-100. Is it really true that the main source (on a mass basis) for Fe, Cu and Mn is combustion? Is there a reference? Seems like road dust/tire and brake wear would be important as well as mineral dust. A more comprehensive assessment of the source of PM2.5 TMI in this study would also be useful given the conclusions (lines 277-285). Is coal fly ash really the main source for PM2.5 TMI in this region?
The issue of source apportionment analysis of aerosol metal in urban Beijing has been studied extensively. Based on these studies, the aerosol metal such as Fe are mainly crust related (Duan et al., 2012) and the peak concentrations of aerosol Fe and Mn reflected dust pollution caused by vehicle driving in traffic rush hours (Zhao et al., 2021). Aerosol Fe also shows a diurnal variation pattern that is high during the day and low at night, the distribution may be due to the intensive anthropogenic activities as

well as the driving of vehicles tire and brake wear in daytime causing elements from surface dust source entering $PM_{2.5}$ (Zhao et al., 2021). Cu and Mn are mainly from non-exhaust emissions of vehicles, fossil fuel combustion or metallurgy (Alexander et al., 2009; Duan et al., 2012; Zhao et al., 2021). Cu and Mn shows no seasonal pattern based on the studies of Zhao et al. (2021) while refers to Duan et al. (2012), higher concentration of Cu in winter indicating sources of coal combustion for heating in Beijing urban. Other studies also pointed out that combustion is an important source of aerosol Cu (Alexander et al., 2009; Schleicher et al., 2011). In the revised MS, we added other sources in addition to the combustion as "Atmospheric anthropogenic sources of transition metals such as iron (Fe) are mainly crust related and the peak concentration of Fe in Beijing is correlated to the vehicle driving in traffic rush hours. Copper (Cu), and manganese (Mn) are mainly from non-exhaust emissions of vehicles, fossil fuel combustion or metallurgy (Alexander et al., 2009; Duan et al., 2012; Zhao et al., 2021)."

On line 277-285, we changed the conclusion as "Compared to the gas-phase oxidants, the control of anthropogenic emissions of aerosol TMI is conducive to the reduction of secondary sulfates. The promotion of clean energy strategies aiming at reducing coal burning and vehicle emissions to improve air quality in North China has reduced not only the primary emissions of SO_2 but also the anthropogenic emissions of aerosol TMIs (Liu et al., 2018) and thus the production of secondary sulfate. What' more, China's ecological and environmental protection measures for tree planting and afforestation are conducive to reducing the generation of dust especially in the spring can further reducing the quality of metal Fe concentrations in aerosols."

10 What are the units for data in table S9?

The unit of metal concentration is ng/m^3 in Table S9. We added the unit is the revised Supplementary Information:

Table S9. Concentration of transition metals in $PM_{2.5}$ in urban areas.

Sampling site	Period	Method	Fe (ng/m^3)	Mn (ng/m^3)	Cu (ng/m^3)	References
China, Beijing, Urban	2018.8-2019.8	XRF	596	27.9	7.37	Zhao et al. (2021)
China, Beijing, Urban	2015.9-2016.1	XRF	686	60.2	25.1	Zhang et al. (2019)
China, Beijing, Urban	2016.6-2017.5	ED-XRF	738	37	32	Cui et al. (2019)
China, Beijing, Urban	2014.1-10	ICP-AES	1650	55	108	Gao et al. (2018)
China, Beijing, Urban	2016.1-2017.5	XRF	629	32	24	Cui et al. (2020)
China, Beijing, Urban	2016.1	ICP-AES	2823	92.3	48	Duan et al. (2012)
China,	2017.10-	XRF	1361	157	29.2	He et al. (2019)

Zhengzhou, Urban	2018.7					
China, Nanjing, Urban	2016.12-2017.12	XRF	577	48.9	27.2	Yu et al. (2019b)
China, Shanghai, Urban	2016.3-2017.2	ED-XRF	410	32	12	Chang et al. (2017)
Canada, Hamilton, Urban	2014.1-2017.6	XRF	49.6	0.83	2.76	Sofowote et al. (2019)
India, New Delhi, Urban	2013.1-2016.12	WD-XRF	780	10	100	Jain et al. (2020)

11 Fig 1 caption needs work; does plot (c) really show diurnal trends, keep same scale for SO4 in (c) and (d), and define SOR and indicate it is the line in plots (e and (f)).

Figure 1 shows the three-hour averaged sulfate formation rates during haze periods in the scale of 6 days. We added the modeled SO_4^{2-} concentration in summer haze periods in panel (d) in the revised MS as shown in the following response. In the section 2.2 the second paragraph, SOR is defined as the ratio of mole concentration of SO_2 to the sum of SO_2 and SO_4^{2-}.

"Compared to the total Fe concentration, it is more effective to evaluate the impact of αFe (III) on sulfate formation. The relationship between αFe (III) and SOR ($\equiv n(SO_2)/n(SO_2+SO_4^{2-})$, defined as the ratio of mole concentration of SO_2 with the sum of SO_2 and SO_4^{2-} mole concentrations) in…"

And we changed the Figure 1 in the revised MS as:

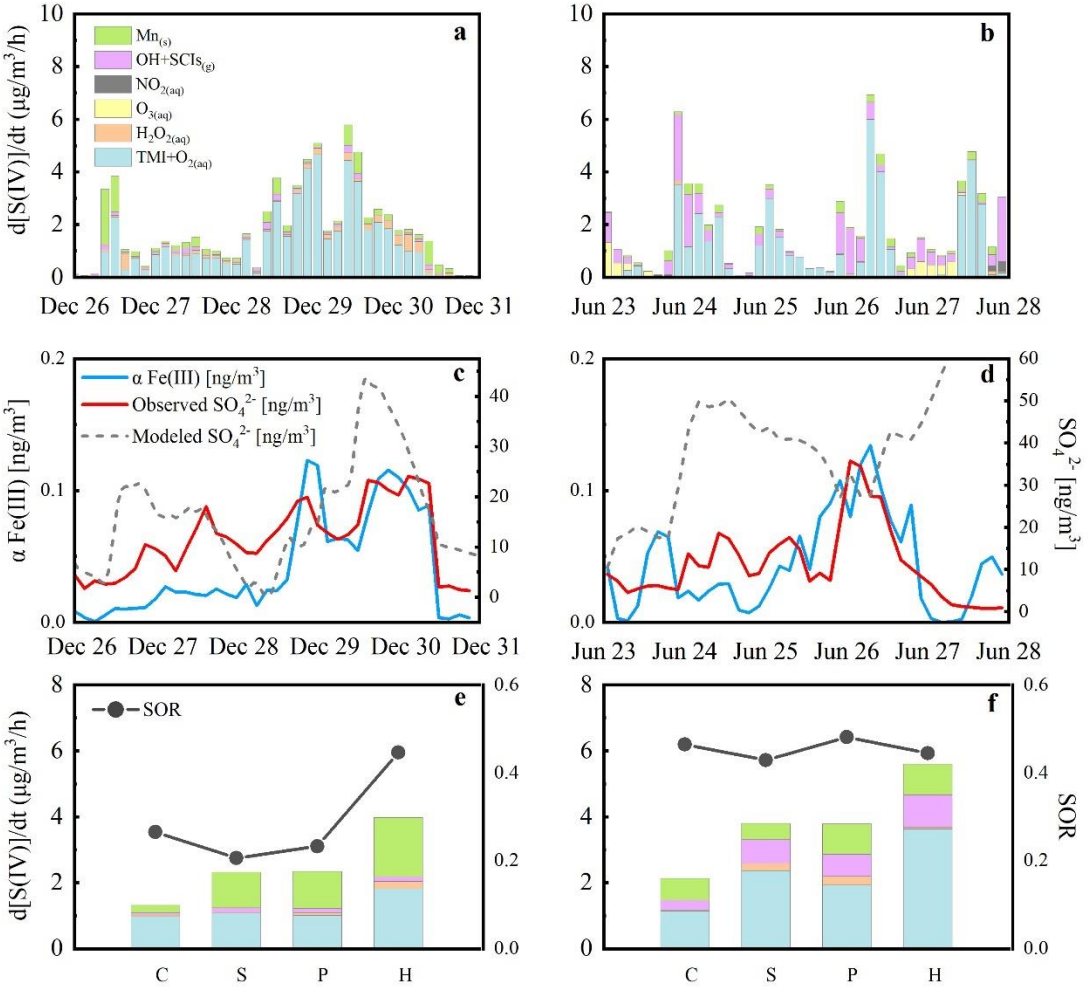

Figure 1. Three-hour average sulfate formation rates during haze periods in winter and summer (a)&(b), corresponding effective Fe (III) concentrations and sulfate concentrations (c)&(d), sulfate formation rates (the histogram) and SOR (the dotted lines) in different pollution levels in two field campaigns (e)&(f).

12 Line 150-151, correlation is not causation, reword to say the correlation is consistent with…

We revised the incorrect statement about the relevant in the revised MS section 2.2 as "Obvious correlations between αFe (III) and sulfate concentration shown in **Fig. 1 (c) and (d)** were observed in the haze periods both in summer (R^2=0.63) and winter (R^2=0.71) and the correlation is consistent with the important contributions from aqTMI pathway to the sulfate formation."

13 Line 153, what does n(SO2) mean?

The definition of n(SO_2) in the MS is the mole concentration of SO_2, and n(SO_2+SO_4^{2-}) is defined as the sum of mole concentration of SO_2 and SO_4^{2-}. We added this piece of definition in the revised MS in section 2.2 as "The relationship between αFe (III) and SOR (≡n(SO_2)/n(SO_2+SO_4^{2-}), defined as the ratio of mole concentration of SO_2 with

the sum of SO_2 and SO_4^{2-} mole concentrations) in PKU-17 winter field campaign was shown in **SI Figure S5**"

14 It should be stated that Eq(1) is simply the conversion of sulfate formation rate in the aerosol water (ie, per mL water) to sulfate formation per m3 of air. There is nothing special about this.

That's true about the comment on Equation (1). Anyway, using different units to look at the rate of sulfate formation is of vital importance to the study of the formation of secondary sulfate aerosols, which can help us better think about the proportion of the contributions from different pathways in different chemical regime. In the revised MS, we added the sentences above the Equation (1) as "In the calculation, we changed the unit of sulfate formation rate from $\mu g/m^3_{air}$ to $mol/s \cdot L_{water}$ and the sulfate formation rate can be calculated via the following equation with the modeled $\frac{dS(VI)}{dt}$ (M/s):…"

15 Line 186-187 and on is not clear. Is the point that the equilibrium amount of H2O2, O3, and NO2 in units of mass/m3 air is controlled by the amount of ALW, ie there is equilibrium between gas and particle water for these oxidants formed in the gas phase. Is the idea that TMI is a primary aerosol (that is not likely really true, it may be true for the total elements, Fe, or Mn, but not the ions) so does not depend on ALW? So the idea is that ALW does not affect TMI levels in solution by affecting the solubility of the overall metal form of the specific species (ie, fig 3 shows insensitivity of pH to ALW, which has been pointed out in other papers (eg, Wong,et al., 2020, Env Sci Tech, 54: 7088-96.)

It was accurately the meaning of line 186-187 and we changed the sentences below the Equation (1) in the revised MS and added the reference to explain the irrelevance of aerosol pH with ALWC.

"The equilibrium amount of H_2O_2, O_3, and NO_2 in units of $\mu g/m^3_{air}$ is controlled by the amount of ALW, ie there is equilibrium between gas and particle water for these oxidants formed in the gas phase. And total amount of metal elements, Fe, Cu or Mn is not dependent on aerosol water content. Aerosol water content does not affect TMI levels in solution by affecting the solubility of the overall metal form of the specific species (**Fig.3** shows insensitivity of pH to ALWC, which has been pointed out in other papers (Wong et al., 2020)."

16 What does $PM_{2.5}$ represent in Fig 3, the total mass including particle water?

The reported $PM_{2.5}$ mass concentration does not include particle water in the original and revised MS. The mass concentration of $PM_{2.5}$ was measured by commercial Ambient Particulate Monitor (TEOM). We added this sentence in the revised MS in Section Methods 1.

17 Line 199-200. What does transition metal mass will not increase mean? The mass concentration of TMI in air or the liquid concentration? Care must be taken in this whole section on what concentration (in air or in ALW) is being discussed.

This part mainly discusses the influence of ALWC on the sulfate formation rates from Mn-surface and aqTMI pathways. Aqueous TMI mole concentration will not increase with the aerosol hygroscopic growth. With the aerosol hygroscopic growth, the increasing of transition metal total mass in air is slower than aerosol water mass in PKU-17. The ratio of Fe total mass with ALWC decreasing with $PM_{2.5}$ mass shown in Fig. S7 indicating a "dilution effect" which means aqueous mole concentration of TMI decreasing with higher aerosol water content. We added the above discussion in Section 2.3 penultimate paragraph in the revised MS as "Due to the obvious heterogeneous reactions contribution to sulfate formation in winter, we evaluated the influence of ALWC on sulfate formation pathways in winter. TMI relevant pathways including aqTMI and Mn-surface pathway were dominate in all range of ALWC as illustrated in **Fig.3**. In PKU-17 field campaign, with the increasing of ALWC from 1 to 150 $\mu g/m^3$, the ratio of Mn-surface/aqTMI continuously decreased mainly because of the decreasing particle specific surface areas. Mn-surface contributed most in lower ALWC range where particle specific surface area was high and provide more reaction positions. Aqueous transition metal ions mole concentration decreasing with the aerosol hygroscopic growth indicating a "dilution effect" as shown in **Fig. S7**. With the aerosol hygroscopic growth, the increasing of transition metal total mass in air is slower than water mass in PKU-17. The ratio of Fe total mass (Fe_t)/ALWC decreasing with $PM_{2.5}$ mass. Previous globle scale observations (Sholkovitz et al., 2012) of ~1100 samples also showed the hyperbolic trends of Fe solubility with total Fe mass. Higher activity coefficients and lower aqueous TMI concentration led to the emergence of "high platform" of the aqTMI pathways contribution to sulfate formation in the range of 50-150 $\mu g/m^3$ ALWC (ie, higher effective aqueous TMI in this range). While ALWC exceeding 150 $\mu g/m^3$in winter, the increase of activity coefficients could not promote the rate of aqTMI. Due to the slight increase of aerosol pH and the dilution effect of aerosol hygroscopic growth on TMI when ALWC exceeding 150 $\mu g/m^3$ as discussed above, the importance of aqTMI and Mn-surface contributions were lowered. At this time, the contributions of external oxidizing substances pathways such as H_2O_2, NO_2 or O_3 may rise in the proper pH range as illustrated in **Fig.4**. In winter fog or cloud conditions with higher water content, the contribution from TMI may decrease a lot for their low solubility and concentrations."

18 Line 200-201. This is not clear and Fig S7 is not clear how it supports this idea of a dilution effect. Define Ft in Fig S7.

The meaning of "dilution effect" was explained in the above response. Fe_t in Fig. S7 means the total mass concentration of $PM_{2.5}$ Fe in air. We changed the title of this figure as: Fig. S7. The "dilution effect" of Fe total mass concentration in air (Fe_t) and ALWC increasing with PM mass in winter and summer.

19 Line 203, it is not clear how the results of Sholkovitz apply here as they are looking at regions largely influenced by mineral dust and some combustion, here the authors state that the metals are from combustion. There is an inconsistency.

We changed the inaccurate statements about the source of aerosol metal including Fe, Cu and Mn in the revised MS, please refer to the above response. Aerosol Fe in Beijing urban area mainly related to the mineral dust and vehicle emissions.

20 Line 204, I do not understand the statement, the importance of aqTMI and Mn-surface contributions were lowered. Why is it lowered, pH in Fig 3 changes very little at ALWC ? 150 ug/m3. This whole section on the effect of water is very confusing. Can the authors give a physical explanation on what the effect of liquid water is on the ambient air concentration of transition metal ions in $PM_{2.5}$.

Aerosol liquid water content has tiny influence on the ambient air total mass transition metal in $PM_{2.5}$ while has the "dilution effect" as discussed above and influence the aqueous TMI concentrations. At the same time, the activity coefficient of TMI increase with aerosol hygroscopic growth led to the emergence of high platforms of the aqTMI pathways contribution to sulfate formation in the range of 50-150 μg/m^3 ALWC. With ALWC exceeding 150 μg/m^3, the effective aqueous TMI concentration (the product of TMI mole concentrations and activity coefficients) decreasing otherwise weaken the importance of aqTMI and Mn-surface. When considering the liquid-phase kinetic reaction to produce sulfate, we pay more attention to the change of the liquid-phase ion concentration in aerosol water rather than the change of the total concentration in the air. We reword this paragraph in the revised MS as mentioned in Response 17.

21 Fig 4 should have plots labeled (a) and (b)

We added the icons in the Figure 4 in the revised MS as follows:

Figure 4. Bar graph showing modelled contributions of various pathways to sulfate formation under different pollution conditions.

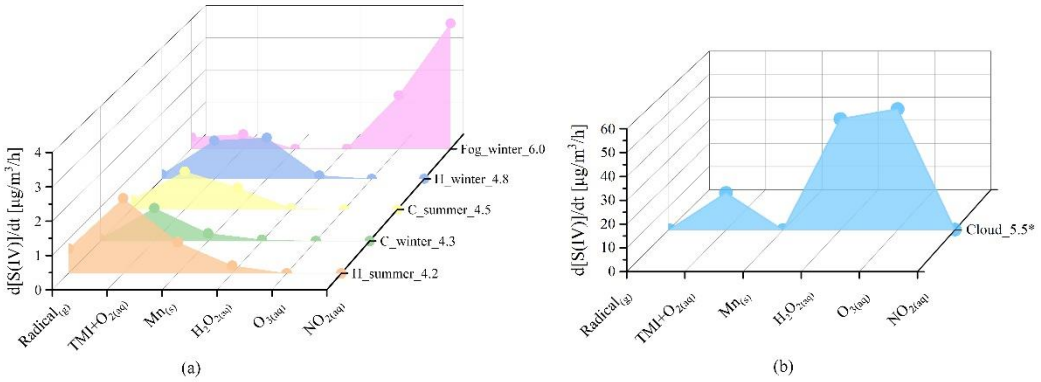

Different pollution conditions including clear ($PM_{2.5}$ smaller than 35 μg/m^3) in winter PKU 2017 (C_winter_4.3) and summer WD 2014 (C_summer_4.5); pollution ($PM_{2.5}$ larger than 75 μg/m^3) in PKU 2017 (H_winter_4.8), WD 2014 (H_summer_4.2); fog conditions used in a previous study(Xue et al., 2016) (Fog_winter_6.0) and cloud conditions (Cloud_5.5) simulated by Seinfeld and Pandis (2016). The number in each

label indicates the average pH value chosen in these calculations. We assumed that the cloud water content is 0.1 g/m^3 in the last condition, and reduced the H_2O_2 concentration to 0.1 ppb compared to the high value used before (Seinfeld and Pandis, 2016).

22 Line 253 to 255 is not clear (While as mentioned above,

In PKU-17 field campaign, with the increasing of ALWC from 1 to 150 $\mu g/m^3$, the ratio of Mn-surface/aqTMI continuously decreased mainly because of the decreasing particle specific surface areas as shown in Fig.3 panel (b) dotted lines. What's more, the organic coating of aerosol particles can largely reduce the reactivity of surface heterogeneous reactions (Zelenov et al., 2017; Anttila et al., 2006; Folkers et al., 2003; Ryder et al., 2015) and may cause the Mn-surface pathway less important. The surface reaction of SO_2 with Mn and other metals in actual aerosol conditions remain unclear, and the relevant calculation results of WD-14 and PKU-17 in this paper represent the upper limit of Mn-surface contribution. We added more references in the revised MS in order to explain the propose of this paragraph:

"While as mentioned above, the ratio of contributions from Mn-surface/aqTMI to produce sulfate will decrease with aerosol hygroscopic growth owning higher ALWC and lower specific surface areas (as shown in Fig.3 panel (b) black dotted line). What's more, the organic coating of aerosol particles can largely reduce the reactivity of surface heterogeneous reactions (Zelenov et al., 2017; Anttila et al., 2006; Folkers et al., 2003; Ryder et al., 2015) and may cause the Mn-surface pathway less important."

23 Line 260-261 reword, not clear.

We reword this part of discussion in the revised MS as follows.

"The organic coating can effectively reduce the reactive sites in the surface of particles hence reduce the reaction probability of SO_2 with surface metal. In the other hand, the widespread presence of aerosol organic coating can also influence the bulk SO_2 catalysed by aqueous TMI but not only the surface reactions. This effect is mainly achieved by the change of SO_2 solubility and diffusion coefficient rather than the rates of catalytic reactions with TMI. Although the solubility of SO_2 in organic solvent changes a lot with the component of organic (Zhang et al., 2013; Huang et al., 2014a), according to previous studies of SO_2 uptake coefficient with sea-salt aerosol (Gebel et al., 2000) and secondary organic aerosol (SOA) (Yao et al., 2019), no obvious uptake coefficient reduction was observed with the organic coating further proving the minor influence of the organic coating on bulk reaction rates. The catalytic reaction of SO_2 with aqTMI may less affected by aerosol organic coating compared to SO_2 with Mn-surface. For these reasons, the surface reaction of SO_2 with Mn and other metals in actual aerosol conditions remain unclear with high uncertainties and need further evaluation. The relevant calculation results of WD-14 and PKU-17 in this paper represent the upper limit of Mn-surface contribution. The missing contribution in WD-14 polluted conditions may mainly come from organic photosensitizing molecules such as HULIS (Wang et al., 2020) under stronger UV in summer or other SOA coupled

mechanisms."

24 Line 324, state-state?

We deleted the incorrect wording "state-state" and changed the sentence as "…the PKU-MARK model produced the concentrations of aqueous reactants in one-hour resolution including…" in the revised MS section 4.2.

Response to the comments of referee #2

The manuscript entitled "A Comprehensive Observational Based Multiphase Chemical Model Analysis of the Sulfur Dioxide Oxidations in both Summer and Winter" by Song et al. presents the comprehensive evaluation of the contribution of different sulfate production pathways in both summer and winter by their self-developed multiphase box model (PKU-MARK). The model includes nearly all the established sulfate production pathways, providing valuable insights into the sulfate formation evaluation. Overall, I have some concerns that need the authors to clarify before that I can recommend publication in Atmospheric Chemistry and Physics.

We thank the reviewer for the helpful comments. The referee's comments are first given in black type, followed by our response to each in turn in blue type. Any changes to the manuscript in response to the comments are then given in quotation marks in red type.

1 The concentration of TMIs is vital in this work since the two dominant sulfate production pathways the authors proposed are aqTMI and Mn-surface. An online monitor measured the Fe and Cu concentrations. Due to the lack of Mn data, the authors propose a fixed ratio of Fe/Mn to stimulate the concentration of Mn. So how about the uncertainty of this method? It is better to compare the concentration of Mn with literature results in the same region.

Under the assumption of fixed Fe/Mn air $PM_{2.5}$ mass concentration ratio as 28, the air mass concentrations of Mn were calculated and shown in Table 1. Mn averaged mass concentration range from 12.4±9.4 ng/m^3 in clean situation to 46.5±10.3 ng/m^3 in highly polluted situation in PKU-17 observation. Compared to measurement results of Mn in the same region reviewed in the Table S9 (27.9 - 92.3 ng/m^3), values were slightly lower. While in the measurements of Cui et al. (2019) in 2016.6 to 2017.5 which is the closest measurement time, averaged Mn concentration was 32±25 ng/m^3 in non-heating periods and 35±36 ng/m^3 in heating periods. The results were in consist with our estimation. However, fixed ratio of Fe/Mn leads to uncertainties of effective aqueous TMI concentration when evaluating the sulfate formation. We have revised the MS to supplement the sensitivity analysis on the concentration of aqueous TMI. Please refer to the response below.

2 The authors state that the average soluble percentage of Fe and Mn in winter polluted conditions was 0.79% and 19.83%. However, the water-soluble fraction of Fe and Mn may change a lot in different regions, as stated in the manuscript. Also, the solubility may change under clean conditions and polluted conditions. It is better to add some discussion about the sensitivity of the solubility of Fe and Mn to the model results.

We added the following discussion of transition metal sensitivity on sulfate formation in PKU-17 winter field campaign in the revised SI Text S4, Figure S9 and Table S10.

Water soluble fraction of Fe, Mn and Cu can vary over a large range. A large part of the

soluble metals is in the form of soluble organic complexes or hydroxides rather than ions in aerosol particles. There are evidences that the existence of various aerosol water soluble organic acids (oxalate, malonate, tartrate and humic acid) cause an enhancement of Fe, Cu and Mn solubility and the formation of metal-organic complex (Paris and Desboeufs, 2013; Wozniak et al., 2015; Tapparo et al., 2020). What's more, the dissolution of Fe and Mn is highly influenced by aerosol pH. Circumneutral pH leads to a supersaturated soluble Fe (III), which then precipitates out of the solution. For these reasons, the promotion of metal solubility may have non-proportional influences on the aqueous concentration TMI. We conducted the sensitivity analysis for the solubility of Fe from 1% to 15% (Scenario one with fixed aqueous Mn and Cu concentration consist with the base run in the MS, Scenario two with fixed ratio of soluble Fe/Mn and Fe/Cu mass, ie, Mn solubility in the range of 10% to 100%, Cu in 5% to 75%, as shown in Table S10). Other aerosol component concentration, ionic strength, ALWC, observed meteorological parameters and trace gases concentrations stay consistent with the base run.

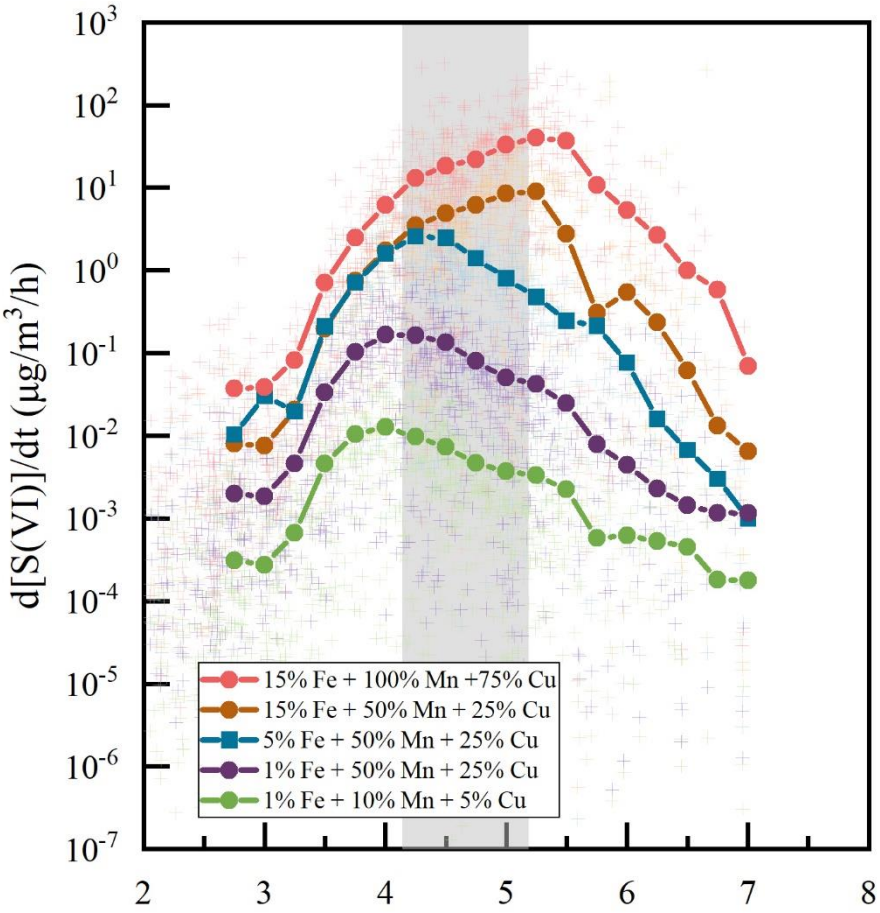

Figure S.9 Sensitivity analysis of transition metal including Fe, Mn and Cu solubility influences on the averaged sulfate formation rates in PKU-17 field observation. Dotted lines in the figure show the cluster averaged results with a pH span of 0.5 under actual ambient conditions with different transition metal solubilities.

Table S10. Base run and scenarios of the solubility sensitivity analysis.

Sensitivity Analysis	Solubility of transition metals	Sulfate formation contribution in haze pH range (4.2-5.2) (μg/m^3/h)
Base Run	5% Fe + 50% Mn + 25% Cu	0.80 - 2.58
Scenario 1	15% Fe + 50% Mn + 25% Cu	3.49 - 8.57
	1% Fe + 50% Mn + 25% Cu	0.05 - 0.16
Scenario 2	15% Fe + 100% Mn + 75% Cu	12.97 - 32.87
	1% Fe + 10% Mn + 5% Cu	0.009 - 0.004

As shown in Figure S.9, In the range of winter haze periods pH (4.2-5.2), averaged sulfate formation rates in PKU-17 field observation is non-proportional to the initial transition metal solubility. Fe solubility increasing from 1% to 5% will cause d[S(VI)]/dt to increase over an order of magnitude, and increasing to 15% cause no obvious effect when pH smaller than 4.2, while obvious effect the pH ranging from 4.2 to 6. This phenomenon may be due to the piecewise calculation equations of TMI-catalysis oxidizing SO_2 as mentioned in the SI and following. In the presence of TMI organic complexes and redox reactions, this equation may need to be further verified, but verification is not within the scope of this study. It is obvious that the d[S(VI)]/dt changes caused by the proportional expansion of the solubility of the three transition metals (Scenario 2) is more significant especially when the solubility is reduced to 1%+10%+5%. Increasing of solubility to 15%Fe+100%Mn+75%Cu can increase sulfate formation rate to 5-84 times higher than in base run during haze periods pH as 4.2-5.2. This can explain to a certain extent that excessive TMI concentrations will not cause a sharp increase in d[S(VI)]/dt, which may be due to the buffering effect caused by the formation of organic complexes.

Part of Table S2. Aqueous-phase reaction rate expressions, rate constants (k) and influence of ionic strength (Is) on k for sulfate production in aerosol particle condensed phase.

Oxidants	The reaction rate expressions ($R_{S(IV)+oxi}$), constants (k) and influence of I_s (in unit of M) on k [a]	Notes	References
TMI+O_2 [f]	$k_6[H^+]^{-0.74}[S(IV)][Mn(II)][Fe(III)]$ (pH ≤ 4.2) $k_6 = 3.72\times10^7\times e^{(-8431.6\times(1/T-1/297))}$ M^{-2} s^{-1} $k_7[H^+]^{0.67}[S(IV)][Mn(II)][Fe(III)]$ (pH > 4.2) $k_7 = 2.51\times10^{13}\times e^{(-8431.6\times(1/T-1/297))}$ M^{-2} s^{-1}		Ibusuki and Takeuchi (1987)
	$\log_{10}(\frac{k}{k^{I_S=0}}) = \frac{b_4\sqrt{I_S}}{1+\sqrt{I_S}}$ [g] b_4 is in range of –4 to –2	$I_{s,\ max}$ = 2 M	Martin and Hill (1987, 1967)

3 The authors declare that their result is consistent with the result of the WRF-CHEM study. However, in the cited work, the ionic strength inhibition effect was not included. More discussion about the results is needed.

In the latest WRF-CHEM study of Tao et al. (2020), the concentrations of Fe and Mn were modeled as the minimum of the solubility of metals regardless of the acidity of aerosol water and ion equilibrium depending on pH. The ionic strength inhibition effect was not included. Using the same Fe/Mn concentration calculation method and considering the ionic strength, Wang et al. (2021) pointed out in the latest research results that aqTMI catalysis only accounts for less than 1% of sulfate formation. Our rough analysis suggests that the calculation method of Fe/Mn may underestimate the actual TMI concentration due to the promotion of metal solubility by organic acid associated with aqTMI concentrations which needs further evaluation and verification. In the revised MS, we deleted the reference of Tao et al. (2020). The influence of ionic strength on the reaction rates were shown in the SI Fig.S1 and discussed in Section 2.1 in the original MS.

4 It is important that the model has considered the activity coefficient values and reactions about oxalate and Fe. So how about the concentration of oxalate used in the model?

Due to the lack of direct measurements in the mentioned field observation campaign, we calculated the aerosol oxalate concentration according to Tao and Murphy (2019) which indicated a mechanisms responsible for the interactions among oxalate, pH, and Fe dissolution in $PM_{2.5}$ based on a long term records in urban and rural areas. The linear regression between monthly average oxalate ($nmol/m^3_{air}$) and water-soluble Fe ($nmol/m^3_{air}$) concentration in $PM_{2.5}$ was fitted as $y=2.89x+0.27$ with R^2 as 0.68. Averaged oxalate aqueous concentration in winter field campaign were 0.55±0.42 in clean period, 0.82±0.48 in slightly polluted period, 0.38±0.29 in polluted period and 0.15±0.16 in highly polluted period with the Fe solubility as 5% in $PM_{2.5}$. We also added the above paragraph in the revised SI Section Text S2.

Other minor comments:

5 Line 11, the wording of sulfate should be better consistent, “sulphate” or “sulfate”.

We changed all word “sulphate” to “sulfate” in the revised MS.

6 Line 13, the statement of “observed concentrations of transition metal ions” is not appropriate from my perspective, given the authors only measured the total concentration of Fe and Cu.

We deleted the words “ions (TMI)” in the revised MS abstract as “…using a state-of-

art multiphase model constrained to the observed concentrations of transition metal, nitrogen dioxide, ozone, …"

7 Line 22, "…affect the environmental quality and human health", references to support this conclusion are lacking.

We added the references in the revised MS as "Secondary sulfate aerosol is an important component of fine particles in severe haze periods (Zheng et al., 2015; Huang et al., 2014b; Guo et al., 2014), which adversely affect the environmental quality and human health (Lippmann and Thurston, 1996; Fang et al., 2017; Shang et al., 2020)."

8 Line 149, "Obvious correlations between alpha-Fe (III) and sulfate…", The author may better calculate the R^2 of alpha-Fe (III) and sulfate.

In four haze periods mentioned in the PKU-17 field campaign, the correlation coefficient R^2 was 0.71, and in WD-14 field campaign haze periods, the coefficient was 0.63 indicating the obvious correlations between aqueous TMI and sulfate formation rates.

In section 2.2 in the revised MS:

"Obvious correlations between αFe (III) and sulfate concentration shown in **Fig. 1 (c) and (d)** were observed in the haze periods both in summer (R^2=0.63) and winter (R^2=0.71) and the correlation is consistent with the important contributions from aqTMI pathway to the sulfate formation."

9 Line 380, in Fig. 1(d), the modeled sulfate concentration line is missing.

We added the modeled sulfate concentration line in the Figure 1 panel (d). Because of the higher boundary layer height and more active lateral boundary conditions in summer, the simulations of secondary sulfate were not in line with observed sulfate concentration. In the section Method 4, we clarified the uncertainties of summer simulated sulfate concentration.

"Due to the higher and more dramatically diurnal changing BLH in summer (Lou et al., 2019), and the lack of relevant data in WD-14 field campaign, we could not get the modelled results of sulfate concentrations in summer haze periods. Direct emissions and transport of sulfate were not considered in the calculation because secondary sulfate is the predominant source in winter haze periods. Dilution was not considered either because the atmosphere is relatively homogeneous during winter haze episodes. Since haze events are normally accompanied by a low boundary layer height (Ht), Ht was set at 300 m at night-time and 450 m at noon (Xue et al., 2016). At other times, Ht was estimated using a polynomial (n = 2) regression as recommended in previous study (Xue et al., 2016). The diurnal trends of sulfate concentrations of the winter haze period using the deposition velocity of 1.5 cm/s and of 2 cm/s in summer are shown in Fig. 1 (c) and (d). Model results had the same trend with the observed values and could explain

the missing source of sulfate aerosol to some extent in winter while with high uncertainties in summer condition."

And Figure 1 in the revised MS:

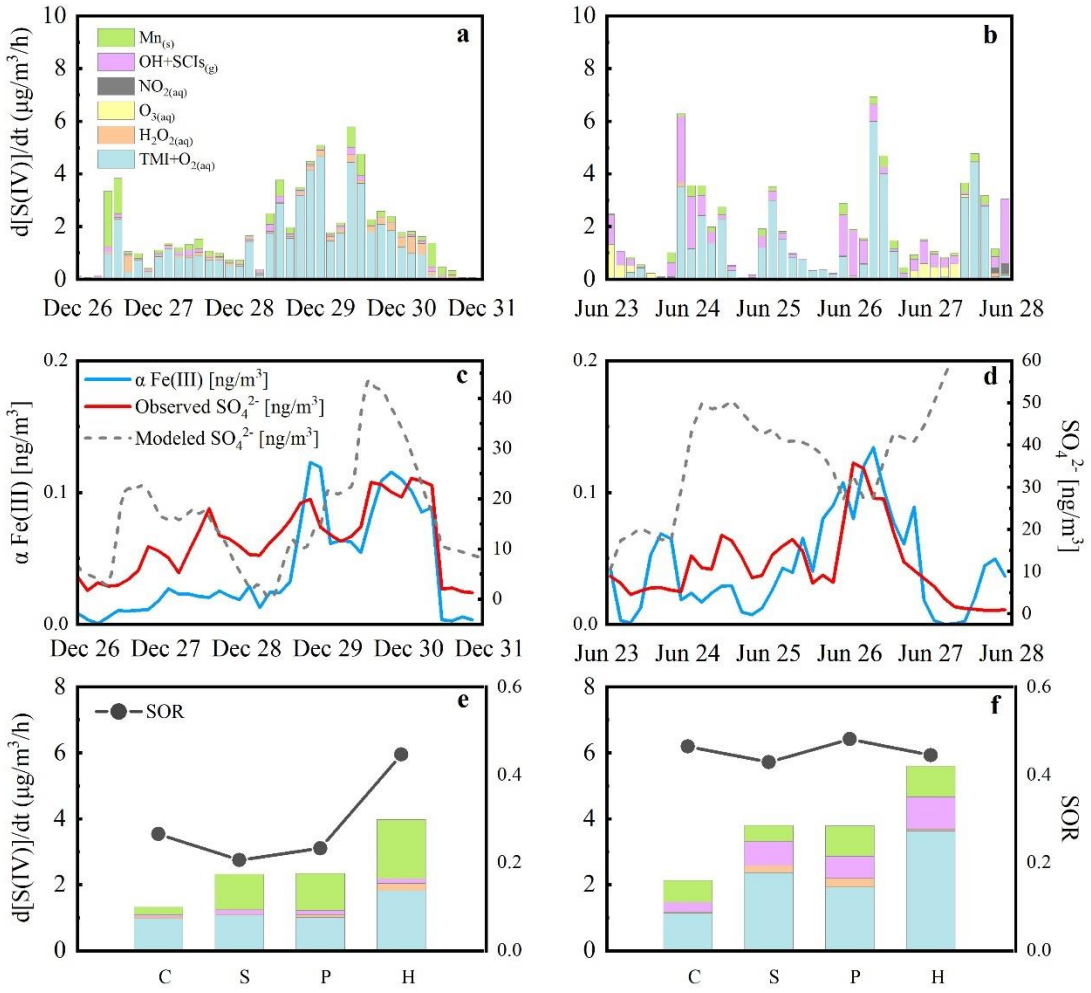

Figure 1. Three-hour average sulfate formation rates during haze periods in winter and summer (a)&(b), corresponding effective Fe (III) concentrations and sulfate concentrations (c)&(d), sulfate formation rates (the histogram) and SOR (the dotted lines) in different pollution levels in two field campaigns (e)&(f).

Reference:

Alexander, B., Park, R. J., Jacob, D. J., and Gong, S.: Transition metal-catalyzed oxidation of atmospheric sulfur: Global implications for the sulfur budget, Journal of Geophysical Research: Atmospheres, 114, https://doi.org/10.1029/2008JD010486, 2009.

Anttila, T., Kiendler-Scharr, A., Tillmann, R., and Mentel, T. F.: On the Reactive Uptake of Gaseous Compounds by Organic-Coated Aqueous Aerosols: Theoretical Analysis and Application to the Heterogeneous Hydrolysis of N2O5, The Journal of Physical Chemistry A, 110, 10435-10443, 10.1021/jp062403c, 2006.

Atkinson, R., Baulch, D. L., Cox, R. A., Crowley, J. N., Hampson, R. F., Hynes, R. G., Jenkin, M. E., Rossi, M. J., and Troe, J.: Evaluated kinetic and photochemical data for atmospheric chemistry: Volume I - gas phase reactions of Ox, HOx, NOx and SOx species, Atmospheric Chemistry and Physics, 4, 1461-1738, 2004.

Baker, A. R. and Jickells, T. D.: Mineral particle size as a control on aerosol iron solubility, Geophysical Research Letters, 33, 10.1029/2006gl026557, 2006.

Baker, A. R., Jickells, T. D., Witt, M., and Linge, K. L.: Trends in the solubility of iron, aluminium, manganese and phosphorus in aerosol collected over the Atlantic Ocean, Marine Chemistry, 98, 43-58, 10.1016/j.marchem.2005.06.004, 2006.

Barth, M. C., Hess, P. G., and Madronich, S.: Effect of marine boundary layer clouds on tropospheric chemistry as analyzed in a regional chemistry transport model, Journal of Geophysical Research: Atmospheres, 107, AAC 7-1-AAC 7-12, https://doi.org/10.1029/2001JD000468, 2002.

Bian, Y. X., Zhao, C. S., Ma, N., Chen, J., and Xu, W. Y.: A study of aerosol liquid water content based on hygroscopicity measurements at high relative humidity in the North China Plain, Atmospheric Chemistry and Physics, 14, 6417-6426, 10.5194/acp-14-6417-2014, 2014.

Chameides, W. and Stelson, A.: Aqueous-phase chemical processes in deliquescent sea-salt aerosols: A mechanism that couples the atmospheric cycles of S and sea salt, Journal of Geophysical Research: Atmospheres, 97, 20565-20580, 1992a.

Chameides, W. L. and Stelson, A. W.: Aqueous-phase chemical processes in deliquescent seasalt aerosols, Ber Bunsen Phys Chem, 96, 461-470, 1992b.

Chang, Y., Huang, K., Deng, C., Zou, Z., Liu, S., and Zhang, Y.: First long-term and near real-time measurement of atmospheric trace elements in Shanghai, China, Atmos. Chem. Phys. Discuss., in Review, 2017.

Cheng, Y., Zheng, G., Wei, C., Mu, Q., Zheng, B., Wang, Z., Gao, M., Zhang, Q., He, K., Carmichael, G., Pöschl, U., and Su, H.: Reactive nitrogen chemistry in aerosol water as a source of sulfate during haze events in China, Science Advances, 2, e1601530, 10.1126/sciadv.1601530, 2016.

Cui, Y., Ji, D., He, J., Kong, S., and Wang, Y.: In situ continuous observation of hourly elements in PM2. 5 in urban beijing, China: Occurrence levels, temporal variation, potential source regions and health risks, Atmos. Environ., 222, 117164, 2020.

Cui, Y., Ji, D., Chen, H., Gao, M., Maenhaut, W., He, J., and Wang, Y.: Characteristics and sources of hourly trace elements in airborne fine particles in urban Beijing, China, Journal of Geophysical Research: Atmospheres, 124, 11595-11613, 2019.

Dong, Z., Su, F., Zhang, Z., and Wang, S.: Observation of chemical components of PM2.5 and secondary inorganic aerosol formation during haze and sandy haze days in Zhengzhou, China, Journal of Environmental Sciences, 88, 316-325, https://doi.org/10.1016/j.jes.2019.09.016, 2020.

Duan, J. C., Tan, J. H., Wang, S. L., Hao, J. M., and Chail, F. H.: Size distributions and sources of

elements in particulate matter at curbside, urban and rural sites in Beijing, Journal of Environmental Sciences, 24, 87-94, 10.1016/s1001-0742(11)60731-6, 2012.
Fang, T., Guo, H., Zeng, L., Verma, V., Nenes, A., and Weber, R. J.: Highly Acidic Ambient Particles, Soluble Metals, and Oxidative Potential: A Link between Sulfate and Aerosol Toxicity, Environ. Sci. Technol., 51, 2611-2620, 10.1021/acs.est.6b06151, 2017.
Farahani, V. J., Soleimanian, E., Pirhadi, M., and Sioutas, C.: Long-term trends in concentrations and sources of PM2.5–bound metals and elements in central Los Angeles, Atmos. Environ., 253, 118361, https://doi.org/10.1016/j.atmosenv.2021.118361, 2021.
Folkers, M., Mentel, T. F., and Wahner, A.: Influence of an organic coating on the reactivity of aqueous aerosols probed by the heterogeneous hydrolysis of N2O5, Geophysical Research Letters, 30, https://doi.org/10.1029/2003GL017168, 2003.
Fountoukis, C. and Nenes, A.: ISORROPIA II: a computationally efficient thermodynamic equilibrium model for K^+-Ca^{2+}-Mg^{2+}-NH_4^+-Na^+-SO_4^{2-}-NO_3^--Cl^--H2O aerosols, Atmospheric Chemistry and Physics Discussions, 7, 1893-1939, 2007.
Gao, J., Peng, X., Chen, G., Xu, J., Shi, G.-L., Zhang, Y.-C., and Feng, Y.-C.: Insights into the chemical characterization and sources of $PM_{2.5}$ in Beijing at a 1-h time resolution, Sci. Total Environ., 542, 162-171, 2016.
Gao, J., Wang, K., Wang, Y., Liu, S., Zhu, C., Hao, J., Liu, H., Hua, S., and Tian, H.: Temporal-spatial characteristics and source apportionment of PM2. 5 as well as its associated chemical species in the Beijing-Tianjin-Hebei region of China, Environ. Pollut., 233, 714-724, 2018.
Gebel, M. E., Finlayson-Pitts, B. J., and Ganske, J. A.: The uptake of SO2 on synthetic sea salt and some of its components, Geophysical Research Letters, 27, 887-890, https://doi.org/10.1029/1999GL011152, 2000.
Goliff, W. S. and Stockwell, W. R.: The regional atmospheric chemistry mechanism, version 2, an update, International con-ference on Atmospheric Chemical Mechanisms, University of California, Davis, 96, 36, 2008.
Goliff, W. S., Stockwell, W. R., and Lawson, C. V.: The regional atmospheric chemistry mechanism, version 2, Atmos. Environ., 68, 174-185, 2013.
Guo, H., Weber, R. J., and Nenes, A.: High levels of ammonia do not raise fine particle pH sufficiently to yield nitrogen oxide-dominated sulfate production, Sci Rep-Uk, 7, 12109, 10.1038/s41598-017-11704-0, 2017.
Guo, H., Xu, L., Bougiatioti, A., Cerully, K. M., Capps, S. L., Hite, J. R., Carlton, A. G., Lee, S. H., Bergin, M. H., Ng, N. L., Nenes, A., and Weber, R. J.: Fine-particle water and pH in the southeastern United States, Atmospheric Chemistry and Physics, 15, 5211-5228, 10.5194/acp-15-5211-2015, 2015.
Guo, S., Hu, M., Zamora, M. L., Peng, J. F., Shang, D. J., Zheng, J., Du, Z. F., Wu, Z., Shao, M., Zeng, L. M., Molina, M. J., and Zhang, R. Y.: Elucidating severe urban haze formation in China, Proceedings of the National Academy of Sciences of the United States of America, 111, 17373-17378, 10.1073/pnas.1419604111, 2014.
Hanson, D. R., Ravishankara, A. R., and Solomon, S.: Heterogeneous reactions in sulfuric-acid aerosol: A framework for model calculations, J. Geophys. Res.-Atmos., 99, 3615-3629, 10.1029/93jd02932, 1994.
He, P., Alexander, B., Geng, L., Chi, X., Fan, S., Zhan, H., Kang, H., Zheng, G., Cheng, Y., and Su, H.: Isotopic constraints on heterogeneous sulfate production in Beijing haze, Atmospheric Chemistry and Physics, 18, 5515-5528, 2018.

He, R.-D., Zhang, Y.-S., Chen, Y.-Y., Jin, M.-J., Han, S.-J., Zhao, J.-S., Zhang, R.-Q., and Yan, Q.-S.: Heavy metal pollution characteristics and ecological and health risk assessment of atmospheric PM2. 5 in a living area of Zhengzhou City, Huan jing ke xue= Huanjing kexue, 40, 4774-4782, 2019.
Heal, M. R., Hibbs, L. R., Agius, R. M., and Beverland, L. J.: Total and water-soluble trace metal content of urban background PM_{10}, $PM_{2.5}$ and black smoke in Edinburgh, UK, Atmos. Environ., 39, 1417-1430, 10.1016/j.atmosphere.2004.11.026, 2005.
Ho, K. F., Lee, S. C., Chan, C. K., Yu, J. C., Chow, J. C., and Yao, X. H.: Characterization of chemical species in PM2.5 and PM10 aerosols in Hong Kong, Atmos. Environ., 37, 31-39, https://doi.org/10.1016/S1352-2310(02)00804-X, 2003.
Hsu, S.-C., Wong, G. T. F., Gong, G.-C., Shiah, F.-K., Huang, Y.-T., Kao, S.-J., Tsai, F., Candice Lung, S.-C., Lin, F.-J., Lin, I. I., Hung, C.-C., and Tseng, C.-M.: Sources, solubility, and dry deposition of aerosol trace elements over the East China Sea, Marine Chemistry, 120, 116-127, https://doi.org/10.1016/j.marchem.2008.10.003, 2010.
Hu, W., Hu, M., Hu, W., Jimenez, J. L., Yuan, B., Chen, W., Wang, M., Wu, Y., Chen, C., Wang, Z., Peng, J., Zeng, L., and Shao, M.: Chemical composition, sources, and aging process of submicron aerosols in Beijing: Contrast between summer and winter, Journal of Geophysical Research: Atmospheres, 121, 1955-1977, https://doi.org/10.1002/2015JD024020, 2016.
Huang, K., Xia, S., Zhang, X.-M., Chen, Y.-L., Wu, Y.-T., and Hu, X.-B.: Comparative Study of the Solubilities of SO2 in Five Low Volatile Organic Solvents (Sulfolane, Ethylene Glycol, Propylene Carbonate, N-Methylimidazole, and N-Methylpyrrolidone), Journal of Chemical & Engineering Data, 59, 1202-1212, 10.1021/je4007713, 2014a.
Huang, R.-J., Zhang, Y., Bozzetti, C., Ho, K.-F., Cao, J.-J., Han, Y., Daellenbach, K. R., Slowik, J. G., Platt, S. M., Canonaco, F., Zotter, P., Wolf, R., Pieber, S. M., Bruns, E. A., Crippa, M., Ciarelli, G., Piazzalunga, A., Schwikowski, M., Abbaszade, G., Schnelle-Kreis, J., Zimmermann, R., An, Z., Szidat, S., Baltensperger, U., Haddad, I. E., and Prévôt, A. S. H.: High secondary aerosol contribution to particulate pollution during haze events in China, Nature, 514, 218-222, 10.1038/nature13774, 2014b.
Huang, X., Song, Y., Zhao, C., Li, M., Zhu, T., Zhang, Q., and Zhang, X.: Pathways of sulfate enhancement by natural and anthropogenic mineral aerosols in China, Journal of Geophysical Research: Atmospheres, 119, 14,165-114,179, https://doi.org/10.1002/2014JD022301, 2014c.
Ibusuki, T. and Takeuchi, K.: Sulfur dioxide oxidation by oxygen catalyzed by mixtures of manganese(II) and iron(III) in aqueous solutions at environmental reaction conditions, Atmospheric Environment (1967), 21, 1555-1560, https://doi.org/10.1016/0004-6981(87)90317-9, 1987.
Ito, A., Myriokefalitakis, S., Kanakidou, M., Mahowald, N. M., Scanza, R. A., Hamilton, D. S., Baker, A. R., Jickells, T., Sarin, M., Bikkina, S., Gao, Y., Shelley, R. U., Buck, C. S., Landing, W. M., Bowie, A. R., Perron, M. M. G., Guieu, C., Meskhidze, N., Johnson, M. S., Feng, Y., Kok, J. F., Nenes, A., and Duce, R. A.: Pyrogenic iron: The missing link to high iron solubility in aerosols, Science Advances, 5, eaau7671, 10.1126/sciadv.aau7671, 2019.
Jain, S., Sharma, S., Vijayan, N., and Mandal, T.: Seasonal characteristics of aerosols (PM2. 5 and PM10) and their source apportionment using PMF: a four year study over Delhi, India, Environ. Pollut., 262, 114337, 2020.
Kayee, J., Sompongchaiyakul, P., Sanwlani, N., Bureekul, S., Wang, X., and Das, R.: Metal Concentrations and Source Apportionment of PM2.5 in Chiang Rai and Bangkok, Thailand during

a Biomass Burning Season, ACS Earth and Space Chemistry, 4, 1213-1226, 10.1021/acsearthspacechem.0c00140, 2020.
Koop, T., Luo, B., Tsias, A., and Peter, T.: Water activity as the determinant for homogeneous ice nucleation in aqueous solutions, Nature, 406, 611-614, 2000.
Lai, S., Zhao, Y., Ding, A., Zhang, Y., Song, T., Zheng, J., Ho, K. F., Lee, S.-c., and Zhong, L.: Characterization of PM2.5 and the major chemical components during a 1-year campaign in rural Guangzhou, Southern China, Atmos. Res., 167, 208-215, https://doi.org/10.1016/j.atmosres.2015.08.007, 2016.
Lelieveld, J. and Crutzen, P. J.: The role of clouds in tropospheric photochemistry, J Atmos Chem, 12, 229-267, 10.1007/bf00048075, 1991.
Li, H. M., Wang, Q. G., Yang, M., Li, F. Y., Wang, J. H., Sun, Y. X., Wang, C., Wu, H. F., and Qian, X.: Chemical characterization and source apportionment of PM2.5 aerosols in a megacity of Southeast China, Atmos. Res., 181, 288-299, 10.1016/j.atmosres.2016.07.005, 2016.
Li, J., Zhang, Y.-L., Cao, F., Zhang, W., Fan, M., Lee, X., and Michalski, G.: Stable Sulfur Isotopes Revealed a Major Role of Transition-Metal Ion-Catalyzed SO_2 Oxidation in Haze Episodes, Environ. Sci. Technol., 54, 2626-2634, 10.1021/acs.est.9b07150, 2020a.
Li, J., Zhu, C., Chen, H., Fu, H., Xiao, H., Wang, X., Herrmann, H., and Chen, J.: A More Important Role for the Ozone-S(IV) Oxidation Pathway Due to Decreasing Acidity in Clouds, Journal of Geophysical Research: Atmospheres, 125, e2020JD033220, https://doi.org/10.1029/2020JD033220, 2020b.
Li, L., Hoffmann, M. R., and Colussi, A. J.: Role of Nitrogen Dioxide in the Production of Sulfate during Chinese Haze-Aerosol Episodes, Environ. Sci. Technol., 52, 2686-2693, 10.1021/acs.est.7b05222, 2018.
Lippmann, M. and Thurston, G. D.: Sulfate concentrations as an indicator of ambient particulate matter air pollution for health risk evaluations, J Expo Anal Environ Epidemiol, 6, 123-146, 1996.
Liu, B., Song, N., Dai, Q., Mei, R., Sui, B., Bi, X., and Feng, Y.: Chemical composition and source apportionment of ambient PM2.5 during the non-heating period in Taian, China, Atmos. Res., 170, 23-33, https://doi.org/10.1016/j.atmosres.2015.11.002, 2016.
Liu, C., Ma, Q., Liu, Y., Ma, J., and He, H.: Synergistic reaction between SO_2 and NO_2 on mineral oxides: a potential formation pathway of sulfate aerosol, Physical Chemistry Chemical Physics, 14, 1668-1676, 10.1039/C1CP22217A, 2012.
Liu, J., Chen, Y., Chao, S., Cao, H., Zhang, A., and Yang, Y.: Emission control priority of $PM_{2.5}$-bound heavy metals in different seasons: A comprehensive analysis from health risk perspective, Sci. Total Environ., 644, 20-30, https://doi.org/10.1016/j.scitotenv.2018.06.226, 2018.
Liu, M., Song, Y., Zhou, T., Xu, Z., Yan, C., Zheng, M., Wu, Z., Hu, M., Wu, Y., and Zhu, T.: Fine particle pH during severe haze episodes in northern China, Geophysical Research Letters, 44, 5213-5221, https://doi.org/10.1002/2017GL073210, 2017.
Liu, P., Ye, C., Xue, C., Zhang, C., Mu, Y., and Sun, X.: Formation mechanisms of atmospheric nitrate and sulfate during the winter haze pollution periods in Beijing: gas-phase, heterogeneous and aqueous-phase chemistry, Atmospheric Chemistry and Physics, 20, 4153-4165, 2020a.
Liu, T., Clegg, S. L., and Abbatt, J. P. D.: Fast oxidation of sulfur dioxide by hydrogen peroxide in deliquesced aerosol particles, Proceedings of the National Academy of Sciences, 117, 1354-1359, 10.1073/pnas.1916401117, 2020b.
Lou, M., Guo, J., Wang, L., Xu, H., Chen, D., Miao, Y., Lv, Y., Li, Y., Guo, X., Ma, S., and Li, J.: On the

Relationship Between Aerosol and Boundary Layer Height in Summer in China Under Different Thermodynamic Conditions, Earth and Space Science, 6, 887-901, https://doi.org/10.1029/2019EA000620, 2019.
Ma, T., Furutani, H., Duan, F., Kimoto, T., Jiang, J., Zhang, Q., Xu, X., Wang, Y., Gao, J., Geng, G., Li, M., Song, S., Ma, Y., Che, F., Wang, J., Zhu, L., Huang, T., Toyoda, M., and He, K.: Contribution of hydroxymethanesulfonate (HMS) to severe winter haze in the North China Plain, Atmos. Chem. Phys., 20, 5887-5897, 10.5194/acp-20-5887-2020, 2020.
Ma, X., Tan, Z., Lu, K., Yang, X., Liu, Y., Li, S., Li, X., Chen, S., Novelli, A., and Cho, C.: Winter photochemistry in Beijing: Observation and model simulation of OH and HO_2 radicals at an urban site, Sci. Total Environ., 685, 85-95, 2019.
Mahowald, N. M., Baker, A. R., Bergametti, G., Brooks, N., Duce, R. A., Jickells, T. D., Kubilay, N., Prospero, J. M., and Tegen, I.: Atmospheric global dust cycle and iron inputs to the ocean, Global Biogeochemical Cycles, 19, https://doi.org/10.1029/2004GB002402, 2005.
Martin, L. R. and Hill, M. W.: The iron catalyzed oxidation of sulfur: Reconciliation of the literature rates, Atmospheric Environment (1967), 21, 1487-1490, 1967.
Martin, L. R. and Hill, M. W.: The effect of ionic strength on the manganese catalyzed oxidation of sulfur (IV), Atmospheric Environment (1967), 21, 2267-2270, 1987.
Ming, L. L., Jin, L., Li, J., Fu, P. Q., Yang, W. Y., Liu, D., Zhang, G., Wang, Z. F., and Li, X. D.: PM2.5 in the Yangtze River Delta, China: Chemical compositions, seasonal variations, and regional pollution events, Environ. Pollut., 223, 200-212, 10.1016/j.envpol.2017.01.013, 2017.
Moch, J. M., Dovrou, E., Mickley, L. J., Keutsch, F. N., Cheng, Y., Jacob, D. J., Jiang, J., Li, M., Munger, J. W., and Qiao, X.: Contribution of hydroxymethane sulfonate to ambient particulate matter: A potential explanation for high particulate sulfur during severe winter haze in Beijing, Geophysical Research Letters, 45, 11,969-911,979, 2018.
Oakes, M., Rastogi, N., Majestic, B. J., Shafer, M., Schauer, J. J., Edgerton, E. S., and Weber, R. J.: Characterization of soluble iron in urban aerosols using near-real time data, Journal of Geophysical Research: Atmospheres, 115, https://doi.org/10.1029/2009JD012532, 2010.
Paris, R. and Desboeufs, K. V.: Effect of atmospheric organic complexation on iron-bearing dust solubility, Atmos. Chem. Phys., 13, 4895-4905, 10.5194/acp-13-4895-2013, 2013.
Petters, M. D. and Kreidenweis, S. M.: A single parameter representation of hygroscopic growth and cloud condensation nucleus activity, Atmos. Chem. Phys., 7, 1961-1971, 10.5194/acp-7-1961-2007, 2007.
Ross, H. B. and Noone, K. J.: A numerical investigation of the destruction of peroxy radical by cu ion catalyzed-reactions on atmospheric particles, J Atmos Chem, 12, 121-136, 10.1007/bf00115775, 1991.
Ryder, O. S., Campbell, N. R., Morris, H., Forestieri, S., Ruppel, M. J., Cappa, C., Tivanski, A., Prather, K., and Bertram, T. H.: Role of Organic Coatings in Regulating N2O5 Reactive Uptake to Sea Spray Aerosol, The Journal of Physical Chemistry A, 119, 11683-11692, 10.1021/acs.jpca.5b08892, 2015.
Sander, R.: Modeling atmospheric chemistry: Interactions between gas-phase species and liquid cloud/aerosol particles, Surveys in Geophysics, 20, 1-31, 1999.
Sarwar, G., J. Godowitch, K. Fahey, J. Xing, David-C Wong, Jeff Young, S. Roselle, AND R. Mathur: Examination of Sulfate production by CB05TU, RACM2 & RACM2 with SCI initiated SO_2,oxidation in the Northern Hemisphere, Presented at Presentation at the CMAS Conference,Chapel Hill, NC2013.

Schleicher, N. J., Norra, S., Chai, F., Chen, Y., Wang, S., Cen, K., Yu, Y., and Stüben, D.: Temporal variability of trace metal mobility of urban particulate matter from Beijing – A contribution to health impact assessments of aerosols, Atmos. Environ., 45, 7248-7265, https://doi.org/10.1016/j.atmosenv.2011.08.067, 2011.

Schwartz, S. E.: Gas phase and aqueous phase chemistry of HO_2 in liquid water clouds, J. Geophys. Res.-Atmos., 89, 1589-1598, 10.1029/JD089iD07p11589, 1984.

Schwartz, S. E.: Mass-transport considerations pertinent to aqueous phase reactions of gases in liquid-water clouds, in: Chemistry of multiphase atmospheric systems, Springer, 415-471, 1986.

Seigneur, C. and Saxena, P.: A theoretical investigation of sulfate formation in clouds, Atmospheric Environment (1967), 22, 101-115, https://doi.org/10.1016/0004-6981(88)90303-4, 1988.

Seinfeld, J. H. and Pandis, S. N.: Atmospheric chemistry and physics: from air pollution to climate change, John Wiley & Sons2016.

Shang, D., Peng, J., Guo, S., Wu, Z., and Hu, M.: Secondary aerosol formation in winter haze over the Beijing-Tianjin-Hebei Region, China, Frontiers of Environmental Science & Engineering, 15, 34, 10.1007/s11783-020-1326-x, 2020.

Shao, J., Chen, Q., Wang, Y., Lu, X., He, P., Sun, Y., Shah, V., Martin, R. V., Philip, S., Song, S., Zhao, Y., Xie, Z., Zhang, L., and Alexander, B.: Heterogeneous sulfate aerosol formation mechanisms during wintertime Chinese haze events: air quality model assessment using observations of sulfate oxygen isotopes in Beijing, Atmos. Chem. Phys., 19, 6107-6123, 10.5194/acp-19-6107-2019, 2019.

Shi, Q., Tao, Y., Krechmer, J. E., Heald, C. L., Murphy, J. G., Kroll, J. H., and Ye, Q.: Laboratory Investigation of Renoxification from the Photolysis of Inorganic Particulate Nitrate, Environ. Sci. Technol., 55, 854-861, 10.1021/acs.est.0c06049, 2021.

Shi, Z., Krom, M. D., Jickells, T. D., Bonneville, S., Carslaw, K. S., Mihalopoulos, N., Baker, A. R., and Benning, L. G.: Impacts on iron solubility in the mineral dust by processes in the source region and the atmosphere: A review, Aeolian Research, 5, 21-42, https://doi.org/10.1016/j.aeolia.2012.03.001, 2012.

Sholkovitz, E. R., Sedwick, P. N., Church, T. M., Baker, A. R., and Powell, C. F.: Fractional solubility of aerosol iron: Synthesis of a global-scale data set, Geochimica et Cosmochimica Acta, 89, 173-189, https://doi.org/10.1016/j.gca.2012.04.022, 2012.

Sofowote, U. M., Di Federico, L. M., Healy, R. M., Debosz, J., Su, Y., Wang, J., and Munoz, A.: Heavy metals in the near-road environment: Results of semi-continuous monitoring of ambient particulate matter in the greater Toronto and Hamilton area, Atmospheric Environment: X, 1, 100005, 2019.

Song, H., Chen, X., Lu, K., Zou, Q., Tan, Z., Fuchs, H., Wiedensohler, A., Zheng, M., Wahner, A., Kiendler-Scharr, A., and Zhang, Y.: Influence of aerosol copper on HO_2 uptake: A novel parameterized equation, Atmos. Chem. Phys. Discuss., 2020, 1-23, 10.5194/acp-2020-218, 2020.

Tan, Z. F., Fuchs, H., Lu, K. D., Hofzumahaus, A., Bohn, B., Broch, S., Dong, H. B., Gomm, S., Haseler, R., He, L. Y., Holland, F., Li, X., Liu, Y., Lu, S. H., Rohrer, F., Shao, M., Wang, B. L., Wang, M., Wu, Y. S., Zeng, L. M., Zhang, Y. S., Wahner, A., and Zhang, Y. H.: Radical chemistry at a rural site (Wangdu) in the North China Plain: observation and model calculations of OH, HO_2 and RO_2 radicals, Atmospheric Chemistry and Physics, 17, 663-690, 10.5194/acp-17-663-2017, 2017.

Tao, W., Su, H., Zheng, G., Wang, J., Wei, C., Liu, L., Ma, N., Li, M., Zhang, Q., Pöschl, U., and Cheng, Y.: Aerosol pH and chemical regimes of sulfate formation in aerosol water during winter haze in the North China Plain, Atmos. Chem. Phys., 20, 11729-11746, 10.5194/acp-20-11729-2020, 2020.

Tao, Y. and Murphy, J. G.: The Mechanisms Responsible for the Interactions among Oxalate, pH, and Fe Dissolution in PM2.5, ACS Earth and Space Chemistry, 3, 2259-2265, 10.1021/acsearthspacechem.9b00172, 2019.

Tapparo, A., Di Marco, V., Badocco, D., D'Aronco, S., Soldà, L., Pastore, P., Mahon, B. M., Kalberer, M., and Giorio, C.: Formation of metal-organic ligand complexes affects solubility of metals in airborne particles at an urban site in the Po valley, Chemosphere, 241, 125025, https://doi.org/10.1016/j.chemosphere.2019.125025, 2020.

Tseng, Y.-L., Wu, C.-H., Yuan, C.-S., Bagtasa, G., Yen, P.-H., and Cheng, P.-H.: Inter-comparison of chemical characteristics and source apportionment of PM2.5 at two harbors in the Philippines and Taiwan, Sci. Total Environ., 793, 148574, https://doi.org/10.1016/j.scitotenv.2021.148574, 2021.

Wang, G., Zhang, R., Gomez, M. E., Yang, L., Zamora, M. L., Hu, M., Lin, Y., Peng, J., Guo, S., Meng, J., Li, J., Cheng, C., Hu, T., Ren, Y., Wang, Y., Gao, J., Cao, J., An, Z., Zhou, W., Li, G., Wang, J., Tian, P., Marrero-Ortiz, W., Secrest, J., Du, Z., Zheng, J., Shang, D., Zeng, L., Shao, M., Wang, W., Huang, Y., Wang, Y., Zhu, Y., Li, Y., Hu, J., Pan, B., Cai, L., Cheng, Y., Ji, Y., Zhang, F., Rosenfeld, D., Liss, P. S., Duce, R. A., Kolb, C. E., and Molina, M. J.: Persistent sulfate formation from London Fog to Chinese haze, Proceedings of the National Academy of Sciences of the United States of America, 113, 13630-13635, 10.1073/pnas.1616540113, 2016a.

Wang, W., Liu, M., Wang, T., Song, Y., Zhou, L., Cao, J., Hu, J., Tang, G., Chen, Z., Li, Z., Xu, Z., Peng, C., Lian, C., Chen, Y., Pan, Y., Zhang, Y., Sun, Y., Li, W., Zhu, T., Tian, H., and Ge, M.: Sulfate formation is dominated by manganese-catalyzed oxidation of SO_2 on aerosol surfaces during haze events, Nature Communications, 12, 1993, 10.1038/s41467-021-22091-6, 2021.

Wang, X., Gemayel, R., Hayeck, N., Perrier, S., Charbonnel, N., Xu, C., Chen, H., Zhu, C., Zhang, L., Wang, L., Nizkorodov, S. A., Wang, X., Wang, Z., Wang, T., Mellouki, A., Riva, M., Chen, J., and George, C.: Atmospheric Photosensitization: A New Pathway for Sulfate Formation, Environ. Sci. Technol., 54, 3114-3120, 10.1021/acs.est.9b06347, 2020.

Wang, Y. N., Jia, C. H., Tao, J., Zhang, L. M., Liang, X. X., Ma, J. M., Gao, H., Huang, T., and Zhang, K.: Chemical characterization and source apportionment of PM2.5 in a semi-arid and petrochemical-industrialized city, Northwest China, Sci. Total Environ., 573, 1031-1040, 10.1016/j.scitotenv.2016.08.179, 2016b.

Weber, R. J., Guo, H., Russell, A. G., and Nenes, A.: High aerosol acidity despite declining atmospheric sulfate concentrations over the past 15 years, Nature Geoscience, 9, 282-285, 10.1038/ngeo2665, 2016.

Welz, O., Savee, J. D., Osborn, D. L., Vasu, S. S., Percival, C. J., Shallcross, D. E., and Taatjes, C. A.: Direct Kinetic Measurements of Criegee Intermediate (CH_2OO) Formed by Reaction of CH_2I with O_2^-, Science, 335, 204-207, 10.1126/science.1213229, 2012.

Wong, J. P. S., Yang, Y., Fang, T., Mulholland, J. A., Russell, A. G., Ebelt, S., Nenes, A., and Weber, R. J.: Fine Particle Iron in Soils and Road Dust Is Modulated by Coal-Fired Power Plant Sulfur, Environ. Sci. Technol., 54, 7088-7096, 10.1021/acs.est.0c00483, 2020.

Wozniak, A. S., Shelley, R. U., McElhenie, S. D., Landing, W. M., and Hatcher, P. G.: Aerosol water soluble organic matter characteristics over the North Atlantic Ocean: Implications for iron-binding ligands and iron solubility, Marine Chemistry, 173, 162-172, https://doi.org/10.1016/j.marchem.2014.11.002, 2015.

Xu, L., Guo, H., Boyd, C. M., Klein, M., Bougiatioti, A., Cerully, K. M., Hite, J. R., Isaacman-VanWertz, G., Kreisberg, N. M., and Knote, C.: Effects of anthropogenic emissions on aerosol formation from

isoprene and monoterpenes in the southeastern United States, Proceedings of the National Academy of Sciences, 112, 37-42, 2015.
Xue, J., Yuan, Z., Griffith, S. M., Yu, X., Lau, A. K. H., and Yu, J. Z.: Sulfate Formation Enhanced by a Cocktail of High NOx, SO_2, Particulate Matter, and Droplet pH during Haze-Fog Events in Megacities in China: An Observation-Based Modeling Investigation, Environ. Sci. Technol., 50, 7325-7334, 10.1021/acs.est.6b00768, 2016.
Yao, M., Zhao, Y., Hu, M. H., Huang, D. D., Wang, Y. C., Yu, J. Z., and Yan, N. Q.: Multiphase Reactions between Secondary Organic Aerosol and Sulfur Dioxide: Kinetics and Contributions to Sulfate Formation and Aerosol Aging, Environmental Science & Technology Letters, 6, 768-774, 10.1021/acs.estlett.9b00657, 2019.
Ye, C., Liu, P., Ma, Z., Xue, C., Zhang, C., Zhang, Y., Liu, J., Liu, C., Sun, X., and Mu, Y.: High H_2O_2 Concentrations Observed during Haze Periods during the Winter in Beijing: Importance of H_2O_2 Oxidation in Sulfate Formation, Environmental Science & Technology Letters, 5, 757-763, 10.1021/acs.estlett.8b00579, 2018.
Yin, L., Niu, Z., Chen, X., Chen, J., Xu, L., and Zhang, F.: Chemical compositions of PM2.5 aerosol during haze periods in the mountainous city of Yong'an, China, Journal of Environmental Sciences, 24, 1225-1233, https://doi.org/10.1016/S1001-0742(11)60940-6, 2012.
Young, L.-H., Li, C.-H., Lin, M.-Y., Hwang, B.-F., Hsu, H.-T., Chen, Y.-C., Jung, C.-R., Chen, K.-C., Cheng, D.-H., and Wang, V.-S.: Field performance of a semi-continuous monitor for ambient $PM_{2.5}$ water-soluble inorganic ions and gases at a suburban site, Atmos. Environ., 144, 376-388, 2016.
Yu, H., Li, W., Zhang, Y., Tunved, P., Dall'Osto, M., Shen, X., Sun, J., Zhang, X., Zhang, J., and Shi, Z.: Organic coating on sulfate and soot particles during late summer in the Svalbard Archipelago, Atmos. Chem. Phys., 19, 10433-10446, 10.5194/acp-19-10433-2019, 2019a.
Yu, Y., He, S., Wu, X., Zhang, C., Yao, Y., Liao, H., Wang, Q. g., and Xie, M.: PM2. 5 elements at an urban site in Yangtze River Delta, China: High time-resolved measurement and the application in source apportionment, Environ. Pollut., 253, 1089-1099, 2019b.
Yue, F., He, P., Chi, X., Wang, L., Yu, X., Zhang, P., and Xie, Z.: Characteristics and major influencing factors of sulfate production via heterogeneous transition-metal-catalyzed oxidation during haze evolution in China, Atmos. Pollut. Res., 11, 1351-1358, https://doi.org/10.1016/j.apr.2020.05.014, 2020.
Zelenov, V. V., Aparina, E. V., Kashtanov, S. A., and Shardakova, E. V.: Kinetics of NO3 uptake on a methane soot coating, Russian Journal of Physical Chemistry B, 11, 180-188, 10.1134/s1990793117010146, 2017.
Zhang, B., Zhou, T., Liu, Y., Yan, C., Li, X., Yu, J., Wang, S., Liu, B., and Zheng, M.: Comparison of water-soluble inorganic ions and trace metals in $PM_{2.5}$ between online and offline measurements in Beijing during winter, Atmos. Pollut. Res., 10, 1755-1765, https://doi.org/10.1016/j.apr.2019.07.007, 2019.
Zhang, N., Zhang, J., Zhang, Y., Bai, J., and Wei, X.: Solubility and Henry's law constant of sulfur dioxide in aqueous polyethylene glycol 300 solution at different temperatures and pressures, Fluid Phase Equilibria, 348, 9-16, https://doi.org/10.1016/j.fluid.2013.03.006, 2013.
Zhang, X., Zhuang, G., Chen, J., Wang, Y., Wang, X., An, Z., and Zhang, P.: Heterogeneous Reactions of Sulfur Dioxide on Typical Mineral Particles, The Journal of Physical Chemistry B, 110, 12588-12596, 10.1021/jp0617773, 2006.
Zhao, D., Song, X., Zhu, T., Zhang, Z., Liu, Y., and Shang, J.: Multiphase oxidation of SO_2 by NO_2 on

$CaCO_3$ particles, Atmos. Chem. Phys., 18, 2481-2493, 10.5194/acp-18-2481-2018, 2018.
Zhao, S., Tian, H., Luo, L., Liu, H., Wu, B., Liu, S., Bai, X., Liu, W., Liu, X., Wu, Y., Lin, S., Guo, Z., Lv, Y., and Xue, Y.: Temporal variation characteristics and source apportionment of metal elements in PM2.5 in urban Beijing during 2018–2019, Environ. Pollut., 268, 115856, https://doi.org/10.1016/j.envpol.2020.115856, 2021.
Zheng, B., Zhang, Q., Zhang, Y., He, K. B., Wang, K., Zheng, G. J., Duan, F. K., Ma, Y. L., and Kimoto, T.: Heterogeneous chemistry: a mechanism missing in current models to explain secondary inorganic aerosol formation during the January 2013 haze episode in North China, Atmos. Chem. Phys., 15, 2031-2049, 10.5194/acp-15-2031-2015, 2015.
Zheng, H., Song, S., Sarwar, G., Gen, M., Wang, S., Ding, D., Chang, X., Zhang, S., Xing, J., Sun, Y., Ji, D., Chan, C. K., Gao, J., and McElroy, M. B.: Contribution of Particulate Nitrate Photolysis to Heterogeneous Sulfate Formation for Winter Haze in China, Environmental Science & Technology Letters, 7, 632-638, 10.1021/acs.estlett.0c00368, 2020.
Zhu, Y., Tilgner, A., Hoffmann, E. H., Herrmann, H., Kawamura, K., Yang, L., Xue, L., and Wang, W.: Multiphase MCM–CAPRAM modeling of the formation and processing of secondary aerosol constituents observed during the Mt. Tai summer campaign in 2014, Atmospheric Chemistry and Physics, 20, 6725-6747, 2020a.
Zhu, Y., Li, W., Lin, Q., Yuan, Q., Liu, L., Zhang, J., Zhang, Y., Shao, L., Niu, H., Yang, S., and Shi, Z.: Iron solubility in fine particles associated with secondary acidic aerosols in east China, Environ. Pollut., 264, 114769, https://doi.org/10.1016/j.envpol.2020.114769, 2020b.

A Comprehensive Observational Based Multiphase Chemical Model Analysis of the Sulfur Dioxide Oxidations in both Summer and Winter

Huan Song[1], Keding Lu[1], Can Ye[1], Huabin Dong[1], Shule Li[1], Shiyi Chen[1], Zhijun Wu[1], Mei Zheng[1], Limin Zeng[1], Min Hu[1] & Yuanhang Zhang[1]*

State Key Joint Laboratory or Environmental Simulation and Pollution Control, College of Environmental Sciences and Engineering, Peking University, Beijing, China

*Correspondence to: Keding Lu; ORCID ID: 12465

Abstract

Sulfate is one of the main components of the haze fine particles and the formation mechanism remains controversial. Lacking of detailed and comprehensive field data hinders the accurate evaluation of relative roles of prevailing sulfate formation pathways. Here, we analysed the sulfate production rates using a state-of-art multiphase model constrained to the observed concentrations of transition metal, nitrogen dioxide, ozone, hydrogen peroxide, and other important parameters in winter and summer in the North China Plain. Our results showed that aqueous TMI-catalysed oxidation was the most important pathway followed by the surface oxidation of Mn in both winter and summer, while the hydroxyl and criegee radicals oxidations contribute significantly in summer. In addition, we also modelled the published cases for the fog and cloud conditions. It is found that nitrogen dioxide oxidation is the dominant pathway for the fog in a higher pH range while hydroperoxide and ozone oxidations dominated for the cloud.

Introduction

Secondary sulfate aerosol is an important component of fine particles in severe haze periods (Zheng et al., 2015; Huang et al., 2014b; Guo et al., 2014), which adversely affect the environmental quality and human health (Lippmann and Thurston, 1996; Fang et al., 2017; Shang et al., 2020). Traditional atmospheric models evaluate secondary sulfate formation via the gas-phase oxidation of sulfur dioxide (SO_2) and a series of multiphase oxidation of dissolved SO_2 in cloud water. During haze events, multiphase oxidation of dissolved SO_2 is more important than SO_2 directly oxidized by gas-phase radicals (Atkinson et al., 2004; Barth et al., 2002) because of the significantly reduced ultraviolet (UV) radiation intensity due to the aerosol dimming effect. Gas-phase reactions,

especially those favouring multiphase chemistry, cannot capture the high concentrations of sulfate aerosols during haze events. Moreover, rapid sulfate production is observed during cloud-free conditions indicating that aerosol multiphase oxidation may be important during haze periods (Moch et al., 2018). These effects cause a major gap between the measured sulfate concentrations under weak UV radiation and the concentrations calculated using traditional atmospheric models.

Assessing the mechanism of multiphase secondary sulfate formation during haze periods helps evaluate the effect of multiphase oxidation. While the gas-phase oxidation rate of SO_2 and OH is well constrained, there are many uncertainties in the quantification of the relative contribution of each multiphase SO_2 oxidation pathway during haze periods. Multiphase oxidation pathways of dissolved SO_2 (Seinfeld and Pandis, 2016; Liu et al., 2020a; Zhu et al., 2020a; Seigneur and Saxena, 1988; Li et al., 2020b) include oxidation by (1) hydrogen peroxide (H_2O_2); (2) ozone (O_3); (3) transition metal ions [TMI, i.e., Fe (III) and Mn (II)] catalysed oxidation pathway (aqTMI)]; and (4) Mn-catalysed oxidation of SO_2 on aerosol surfaces pathway (Mn-surface) (Wang et al., 2021). Some studies (Cheng et al., 2016; Wang et al., 2016a; Xue et al., 2016; Li et al., 2018) also suggested that nitrogen oxides may play a crucial role in the explosive growth of sulfate formation during severe haze days in Beijing because of the high pH near a neutral system, by facilitating the catalysis of mineral dust (Liu et al., 2012; Zhao et al., 2018) or the photolysis of nitrous acid (Zheng et al., 2020). However, the average pH during Beijing haze periods is approximately 4.2 (Liu et al., 2017), and a high level of NH_3 does not increase the aerosol pH sufficiently to yield NO_2-dominated sulfate formation (Guo et al., 2017). Other studies (Ye et al., 2018; Liu et al., 2020b) emphasized the importance of H_2O_2 oxidation to sulfate formation due to the underestimation of H_2O_2 concentrations during haze episodes in previous studies or the influence of high ionic strength (I_s)

of aerosol solutions on the H_2O_2 oxidation rate, which implies that oxidant concentrations for SO_2 oxidation constrained to the observed values from field measurements are required. Previous study (Wang et al., 2020) showed that photosensitization is a new pathway for atmospheric sulfate formation and requires further verification. According to previous studies of the GEOS-Chem model and including the measurements of oxygen isotopes ($\Delta^{17}O$ (SO_4^{2-})) (He et al., 2018; Shao et al., 2019; Li et al., 2020a; Yue et al., 2020), several studies showed that aqTMI was important during some haze periods. Overall, the formation mechanisms of the missing sulfate sources remain unclear and controversial.

Sulfate formation is a complex multiphase physicochemical reaction process, in which parameters have multiple interrelationships. The previous studies have mostly selected typical conditions with fixed parameters for numerical calculations, ignoring the fact that sulfate formation is a complex dynamic process. A comprehensive and explicit evaluation of the sulfate generation process requires real-time feedback and explicit constraints of observational data. Therefore, it is crucial to apply constrained parameters from field campaigns in the calculations. Moreover, as proposed in previous studies (Liu et al., 2020b; Cheng et al., 2016), due to the lower water content in aerosol particles than in cloud water, the non-ideality effects of aerosol solutions should be carefully considered.

In this study, we modelled the concentrations of the main reagents of sulfate formation reactions using a state-of-art Peking-University-Multiple-phAse Reaction Kinetic Model (PKU-MARK) based on the data measured in two field campaigns conducted in the winter and summer in the North China Plain (NCP) where several particle pollutions happened. The non-ideality of aerosol solutions was considered in the calculation of both gas solubility and aqueous-phase reaction rates. Chemical regimes in the aerosol particle bulk phase were analysed to understand the role of gas-phase radical

precursors, particle TMIs, aerosol surface concentrations and the aerosol liquid water content (ALWC) on the aqueous reactant levels and the sulfate formation rate. All particle concentrations reported are fine particle matters particulate matter with aerodynamic diameter of 2.5 μm or less ($PM_{2.5}$).

The overall goal of this work is to evaluate the contribution of different secondary sulfate formation pathways under actual field measurement conditions in the NCP. Effects of non-ideality of condensed particle phase and the solubility of gas-phase reactants on the reactions enable the comparisons with parameters previously obtained in model calculations. In addition, episodes at different pollution levels in the winter and summer campaigns were selected to evaluate the contribution of prevailing sulfate formation pathways proposed in previous studies. As a study evaluating the contribution of different sulfate formation pathways during field campaign observations, this work provides an improved understanding of atmospheric sulfate formation at different pollution levels in the NCP.

2 Results

2.1 Overview of the field observations

Table 1 shows the key meteorological parameters, trace gases concentrations, calculated ALWC, ionic strength, pH and sulfate formation rates under different pollution conditions in PKU-17 and WD-14 comprehensive field campaigns. Sampling location and experimental methods used in these two campaigns are summarized in the Method part. The pollution degree is classified according to the mass concentration of $PM_{2.5}$. The clean condition means $PM_{2.5}$ smaller than 35 μg/m^3, the slightly polluted condition is 35-75 μg/m^3, the polluted condition is 75-150 μg/m^3 and highly polluted is larger than 150 μg/m^3. Sulfate formation rates were modelled by the Multiple-phAse Reaction Kinetic Model (PKU-MARK) (mentioned in Method) with constrained parameters. The effects of aerosol non-ideality were considered in the size-segregated model. Data points with relatively humidity (RH) smaller than 20% and AWLC smaller than 1 μg/m^3 were abandoned to improve the accuracy of the results.

Transition metals concentrations including Fe and Mn increased with PM mass (as shown in Fig.1). Photochemical oxidants including H_2O_2 and O_3 exhibited a decreasing trend with the increase of PM mass because of the significantly reduced solar ultraviolet (UV) radiation intensity due to the aerosol dimming effect. Some studies reported high H_2O_2 concentrations during haze episodes (Ye et al., 2018), whereas in PKU-17 field campaign, the average concentration of H_2O_2 was only 20.9±22.8 pptV in highly polluted conditions. Higher sulfate concentration was observed in the high range of RH and ALWC indicating their enhancement effects on the sulfate formation. We also picked four haze periods in PKU-17 observation, the time series of these key parameters are provided in Supplementary Information **(SI) Fig. S4**.

Aerosol pH values were calculated using the ISORROPIA-II model. The calculated particle pH values as shown in the **Table 1** are in good agreement with the values reported in other studies (Guo et al., 2017; Weber et al., 2016). The lower pH in the range of 4.0–5.5 is beneficial to sulfate formation via aqTMI. Aerosol liquid water is another key component, higher loading of aerosol liquid water is more conducive to the occurrence of multiphase reactions. The ALWC in the PKU-17 and WD-14 campaigns was calculated via the ISORROPIA II model with input concentrations of aerosol inorganic components (see **Method M.3**). Aerosol liquid water did not freeze at winter temperatures below 273 K in the PKU field campaign because of the salt induced freezing point depression (Koop et al., 2000). Wind speeds during these haze events were persistently low (0.3–1.5 m/s), indicating the minor contribution of regional transport to sulfate production.

Aqueous TMI concentration level is crucial in the evaluation of secondary sulfate formation in real atmospheric conditions. Atmospheric anthropogenic sources of transition metals such as iron (Fe) are crust related and the peak concentration of Fe in Beijing is correlated to the vehicle driving in traffic rush hours. Copper (Cu), and manganese (Mn) are mainly from non-exhaust emissions of vehicles, fossil fuel combustion or metallurgy (Alexander et al., 2009; Duan et al., 2012; Zhao et al., 2021). Concentrations of transition metals are highly variable, ranging from <0.1 ng m-3 to >1000 ng m-3 globally (Alexander et al., 2009). Fe solubility in atmospheric aerosols has been reported to range from 0.1% to 80% (Ito et al., 2019; Hsu et al., 2010; Heal et al., 2005; Shi et al., 2012; Mahowald et al., 2005), and elevated levels of Fe solubility have been observed in aerosols dominated by combustion sources. The average fractional Fe solubility in areas away from dust source regions is typically between 5 and 25% (Baker and Jickells, 2006; Baker et al., 2006; Hsu et al., 2010). A recent study reported the average Fe solubility as 2.7–5.0% in Chinese cities, and more

than 65% of nano-sized Fe-containing particles were internally mixed with sulfates and nitrates (Zhu et al., 2020b). The solubility of Mn tends to be higher than that of Fe (Baker et al., 2006), which is 22–57% in urban aerosol particles (Huang et al., 2014c). In this study, we chose the solubility of total Fe as 5% and total Mn solubility as 50% assuming that aerosol particles are internally mixed. In Beijing, high concentrations of Fe, Cu, and Mn were observed (**Table S9**). Concentrations of transition metals are strongly correlated during these haze periods; thus, we propose a fixed ratio of Fe/Mn to account for the lack of Mn data in PKU-17 and WD-14 field campaigns **(SI Text S2)**.

Aerosol trace metal speciation and water solubility are affected by factors such as photochemistry, aerosol pH, and aerosol particle size (Baker and Jickells, 2006; Oakes et al., 2010). Soluble iron in aerosol water exists as Fe (II) and Fe (III), with a series of redox recycling between the two species and other ions. Partitioning between Fe (II) and Fe (III) varies diurnally with the highest fraction of Fe (II) found during the day because of the photochemical reactions reducing Fe (III) to Fe (II). Photolysis reactions of iron hydroxides and organic complexes were documented as the most important source of Fe (II) in cloud and fog water. Oxalic acid and its deprotonated form, oxalate, have strong coordination ability with Fe and form Fe-oxalate complexes, which have higher photochemical activity than Fe hydroxide. All these mechanisms are included in the PKU-MARK model. Diurnal trends of sulfate formation were observed during haze periods indicating the diurnal distribution of different states of iron. Redox cycling of other TMIs such as Cu and Mn are also considered in the PKU-MARK model. Averaged percentage of soluble Fe (III) and Mn (II) was 0.79% and 19.83% in winter polluted conditions and 2.57% and 52.15% in summer polluted conditions. The main reason for the difference between winter and summer metal solubility is that summer

aerosols have higher water content and lower ionic strength, which is conducive to the dissolution of Fe and Mn. The solubility range is in good agreement with the values reported in previous observations (Ito et al., 2019; Hsu et al., 2010).

The influence of aerosol ionic strength on aqTMI reaction rates was considered carefully in the study. Higher ALWC is typically accompanied by lower ionic strength, which increases the activity of TMI. The relationship (Liu et al., 2020b) between the rate coefficients of the TMI pathway and ionic strength is displayed in **Fig. S1**. The sulfate formation rate decreased by 424.82 times when ionic strength was 45 M compared to the dilute solution with ionic strength of 0 M. Despite considering the effect of the activity coefficient on the reaction rate of aqTMI, the contribution of the aqTMI was still dominant during haze periods indicating that the dominance of aqTMI can be a widespread phenomenon, as recommended in previous studies (He et al., 2018; Shao et al., 2019; Li et al., 2020a; Yue et al., 2020).

2.2 Analysis of sulfate formation rate in different pollution conditions

Fig. 1 (a) and (b) display the 3-h averaged sulfate formation rates in the PKU-17 and WD-14 during haze periods. Contributions of the gas-phase radical oxidants were much higher during summer time. To fully explain the relative contributions to sulfate formation from different pathways, the stabilized criegee intermediates (SCIs) oxidant was also considered in the calculations. Based on the previous report (Sarwar, 2013), the inclusion of the SCIs oxidation pathway further enhances sulfate production. We modified the Regional Atmospheric Chemistry Mechanism (RACM2) (Goliff et al., 2013; Goliff and Stockwell, 2008) to represent three explicit SCIs and their subsequent reactions (Welz et al., 2012) with SO_2, NO_2, aldehydes, ketones, water monomer, and water dimmer and calculated the contribution of this pathway in two field campaigns.

The contribution of aqTMI increased rapidly with the aggravated pollution. High concentrations of transition metals observed in Beijing facilitated the dissolution of Fe, Cu, and Mn. The relationship of ionic strength and aqTMI rate constant is illustrated in **SI Fig. S1** and **Table S2** (Liu et al., 2020b). αFe (III) is defined as the product of the Fe (III) activity coefficient, concentration, molecular weight (56) and aerosol liquid water content. Compared to the total Fe concentration, it is more effective to evaluate the impact of αFe (III) on sulfate formation. The relationship between αFe (III) and SOR ($\equiv n(SO_2)/n(SO_2+SO_4^{2-})$, defined as the ratio of mole concentration of SO_2 with the sum of SO_2 and SO_4^{2-} mole concentrations) in PKU-17 winter field campaign was shown in **SI Figure S5**. Because of the inhibition of the effects of high ionic strength on the rate constant of aqTMI, a high volume of aerosol water during the haze event increased the TMI activity coefficient benefiting sulfate formation. Obvious correlations between αFe (III) and sulfate concentration shown in **Fig. 1 (c) and (d)** were observed in the haze periods both in summer (R^2=0.63) and winter (R^2=0.71) and the correlation is consistent with the important contributions from aqTMI pathway to the sulfate formation. Affected by the higher boundary layer height and higher gas phase radical concentration in summer, the correlation between sulfate oxidant ratio SOR and PM mass in summer is not as significant as that in winter. In summer, as illustrated in **Fig. S6**, there was still an obvious positive dependence between SOR and RH and ALWC, whereas a negative correlation was found between SOR and odd-oxygen ($[Ox]\equiv[O_3]+[NO_2]$). As shown in **Fig. 1 (e) and (f)**, the sulfate formation through gaseous reaction was more important in summer than in winter, mainly provided by gas phase radicals (OH and SCIs). In WD-14 field campaign, heterogeneous aqTMI pathways were still dominant in the secondary sulfate formation.

2.3 Dependence of the Secondary sulfate formation rates on aerosol pH and water content

Aerosol pH and ALWC were calculated using the ISORROPIA-II model (Method M3). Because of the high sensitivity of sulfate formation to pH, the lower range of aerosol pH during these two campaigns made the aqTMI the most important one. The effects of high aerosol ionic strength on the dissolution equilibrium and reaction rates were considered in calculations (Liu et al., 2020b) (**SI Table S2 to S4)**. Due to the low H_2O_2 concentration (~0.023 ppbV) and low ALWC observed in the PKU-17 field campaign, the average contribution of H_2O_2 in haze periods ($PM_{2.5}$ > 75 μg/m^3) was about 0.11±0.15 μg/m^3/h. Higher gas-phase H_2O_2 concentration may further increase the contribution of this pathway to sulfate formation. Based on a recent report (Ye et al., 2018), higher gas-phase H_2O_2 concentrations were observed in the NCP during different haze events, including severe haze episodes in suburban areas. At 0.1 ppbV H_2O_2 (about five times higher than the observed H_2O_2 concentration), the calculated sulfate formation rate was 0.52±0.76 μg/m^3/h in haze periods with great uncertainty and still lower than the contribution of the TMI pathway (1.17±1.48 μg/m^3/h).

Due to the potential interaction between various factors in the atmosphere, fixing certain parameters and changing only the pH to obtain the sulfate production rate may cause errors. With the development of haze, concentrations of O_3 and OH radicals decrease due to reduced UV radiation caused by the aerosol dimming effect. Despite its minor contribution to sulfate production in winter, the increase in the ozone oxidation rate with pH was slower under actual conditions. Contributions of gas-phase radicals also showed a weak downward trend in the summer campaign (**Fig. 2 (c))**. The bias between calculated and observed values indicated a dynamic balance of atmospheric oxidation in the gas phase and aerosol phase. If we arbitrarily use the average values during haze periods and only changed the pH of the aerosols as in previous studies, the obtained sulfate

production rate will deviate from the observed values. Actual ambient sulfate formation rates calculated using the measured values in polluted periods in two field campaigns are illustrated in **Fig. 2 (a) and (c)**. Average values except for pH during the haze periods were used to calculate the sulfate formation rates as shown in **Fig. 2 (b) and (d)**. The peak of the H_2O_2 line in the figure is caused by the change in the water content and ionic strength. In the pH range of 4.0–6.0, the calculated ALWC was in the highest range, increasing the contribution of H_2O_2 proportionally as calculated using **equation (1)**.

Aerosol water content is another key factor that influences the contribution of different pathway to sulfate formation. In the calculation, we changed the unit of sulfate formation rate from μg/m^3_{air} to mol/s·L_{water} and the sulfate formation rate can be calculated via the following equation with the modeled $\frac{dS(VI)}{dt}$ (M/s):

$$\frac{dS(VI)}{dt}\ (\mu g\ m^{-3} \cdot h^{-1}) = 0.01 \times 3600\ (s\ h^{-1}) \cdot 96\ g\ mol^{-1} \cdot \frac{dS(VI)}{dt}\ (M\ s^{-1}) \cdot \frac{ALWC}{\rho_{water}} \quad (1)$$

where ALWC is in units of μg m^{-3} and ρ_{water} is the water density in kg L^{-1}. At high ionic strength, this expression is more accurate than the equivalent expression with the unit of M s^{-1}. The equilibrium amount of H_2O_2, O_3, and NO_2 in units of μg/m^3_{air} is controlled by the amount of ALW, ie there is equilibrium between gas and particle water for these oxidants formed in the gas phase. And total amount of metal elements, Fe, Cu or Mn is not dependent on aerosol water content. Aerosol water content does not affect TMI levels in solution by affecting the solubility of the overall metal form of the specific species (**Fig.3** shows insensitivity of pH to ALWC, which has been pointed out in other papers (Wong et al., 2020). The reaction kinetics and rate constants summarized in **Table S2** suggest that there is a proportional relationship between ALWC and sulfate formation pathways except aqTMI. One reason for the lower sulfate formation rate observed in the PKU-17

(1–3 μg m^{-3} h^{-1}) is that the ALWC values were lower than those assumed in previous studies (ALWC = 300 μg m^{-3}). This deviation from the ALWC significantly reduces the contribution of several other pathways, but not the contribution of transition metals to sulfate formation.

Due to the obvious heterogeneous reaction's contribution to sulfate formation in winter, we evaluated the influence of ALWC on sulfate formation pathways in winter. TMI relevant pathways including aqTMI and Mn-surface pathway were dominate in all range of ALWC as illustrated in **Fig.3**. In PKU-17 field campaign, with the increasing of ALWC from 1 to 150 μg/m^3, the ratio of Mn-surface/aqTMI continuously decreased mainly because of the decreasing particle specific surface areas. Mn-surface contributed most in lower ALWC range where particle specific surface area was high and provide more reaction positions. Aqueous transition metal ions mole concentration decreasing with the aerosol hygroscopic growth indicating a "dilution effect" as shown in **Fig. S7** With the aerosol hygroscopic growth, the increasing of transition metal total mass in air is slower than water mass in PKU-17. The ratio of Fe total mass (Fe_t)/ALWC decreasing with $PM_{2.5}$ mass. Previous globle scale observations (Sholkovitz et al., 2012) of ~1100 samples also showed the hyperbolic trends of Fe solubility with total Fe mass. Higher activity coefficients and lower aqueous TMI concentration led to the emergence of "high platform" of the aqTMI pathways contribution to sulfate formation in the range of 50-150 μg/m^3 ALWC (ie, higher effective aqueous TMI in this range). While ALWC exceeding 150 μg/m^3in winter, the increase of activity coefficients could not promote the rate of aqTMI. Due to the slight increase of aerosol pH and the dilution effect of aerosol hygroscopic growth on TMI when ALWC exceeding 150 μg/m^3 as discussed above, the importance of aqTMI and Mn-surface contributions were lowered. At this time, the contributions of external oxidizing substances pathways such as H_2O_2, NO_2 or O_3 may rise in the proper pH range

as illustrated in **Fig.4**. In winter fog or cloud conditions with higher water content, the contribution from TMI may decrease a lot for their low solubility and concentrations.

The same analysis also used in the summer WD-14 field campaign (as shown in **SI Fig.S8**). "The dilution effect" occurred more dramatically in summer compared to that in winter because of a higher RH and higher percentage of water in the aerosol. In this situation, the contribution of aqTMI or Mn-surface was inhibited due to the low soluble TMI concentrations. Considering the positive relationships of SOR and RH in summer WD-14 field campaign, aqueous and surface sulfate formation contributions mentioned in the study could not explain the missing source of secondary sulfate. Because of the low pH range observed in WD-14 field campaign, the contributions from H_2O_2, NO_2, O_3 or NO_3^- photolysis were negligible. The missing contribution may mainly come from other pathways such as photosensitizing molecules (Wang et al., 2020) under stronger UV in summer or contributions from hydroxy methane sulfonate (Moch et al., 2018; Ma et al., 2020) which need further studies.

Discussion and Conclusion

We evaluated the contribution of different pathways to secondary sulfate formation using a state-of-art size-segregated multiphase model constrained to the observed parameters from two field campaigns in the North China Plain. In addition, the effects of aerosol solution non-ideality on aqueous-phase reaction rates as well as dissolution equilibriums were considered in the calculations. The results indicated that the aqueous TMI-catalysed oxidation pathway (aqTMI) was an important contributor to sulfate formation during haze episodes, which is consistent with the results of the isotope and WRF-CHEM studies (He et al., 2018; Shao et al., 2019; Li et al., 2020a; Yue et al., 2020).

Despite the dominant role of aqTMI in PKU-17 field campaign, contributions from other multiphase pathways are not negligible. Dominant pathways varied with conditions such as clear or haze periods in clouds or aerosol water. **Fig. 4** exhibits the contribution of different oxidation pathways to sulfate formation in aerosol water (under different pollution levels), fog, and clouds to indicate the dominant factors of sulfate formation under different conditions. In clear periods, gas-phase oxidation of SO_2 by gas phase radicals (OH and SCIs) happens continuously, contributing 0.01–0.6 $\mu g/m^3/h$ to sulfate formation. At the clean time, sulfate production is mainly limited by relatively low SO_2 concentrations and low ALWC, which has promotion effects on the multiphase sulfate formation pathways. The average sulfate formation rate during clear days was 1.30 $\mu g/m^3/h$ in winter and 2.13 $\mu g/m^3/h$ in summer because of the generally higher ALWC in summer aerosol and much higher gas phase radical concentrations. Gas-phase radicals (OH and SCIs) continuously oxidize SO_2 during the haze and clear periods.

External oxidizing substances such as NO_2 and O_3 had little contribution to sulfate formation during

these haze periods because of the high aerosol acidity. High pH (near 7) values were observed in these field campaigns when the contribution of the NO_2 pathway was dominant at some point but not during the entire pollution process; its proportion was much lower than that of aqTMI. Although the enhancement factor of H_2O_2 oxidation was considered based on the measurement of previous study (Liu et al., 2020b), the contribution of H_2O_2 oxidation was still below 0.5 μg S(VI)/m^3/h because ALWC was about 10 times lower than 300 μg m^{-3}, which was used in previous studies (Cheng et al., 2016; Liu et al., 2020b).

The sulfate formation rate is limited by the ALWC according to **equation (1)**. Aerosol particles have lower water content than cloud droplets, which provides larger space for aqueous phase reactions. Therefore, at the gas-phase SO_2 concentrations of 5–50 ppb, 10–100 times higher water content in fog and cloud droplets can cause higher sulfate formation rates up to 100 μg m^{-3} h^{-1} assuming 0.1 g m^{-3} water in clouds (**Fig. 4)**. A high H_2O_2 concentration (1 ppb), which was 50 times higher than that in the PKU field campaign, was used in the calculation in the Cloud_5.0 regime (Seinfeld and Pandis, 2016). No obvious contribution from the NO_2 oxidation pathway was observed in the PKU-17 and WD-14 field campaigns because of the lower pH range. As proposed in a previous study, the particulate nitrate photolysis can explain the missing source of sulfate in Beijing haze (Zheng et al., 2020). However, according to the recent laboratory report (Shi et al., 2021), the nitrate photolysis enhancement factor is no larger than 2 at all RH ranges. We also included the calculation of nitrate photolysis in this study due to the high loading of particle nitrate and found that the contribution was rather small (~0.008 μg m^{-3} h^{-1} in winter haze periods); thus, we did not include this pathway in the figures.

According to our modelled results and the newest study (Wang et al., 2021), Mn surface reactions

contributed a lot to sulfate formation. Except for possible $Mn(OH)_x^{(3-x)}$ reacting with SO_2, Zhang et al. (2006) proposed that other metal oxides such as Fe_2O_3 and Al_2O_3 can also react with SO_2 on the surface of particles. While as mentioned above, the ratio of contributions from Mn-surface/ aqTMI to produce sulfate will decrease with aerosol hygroscopic growth owning higher ALWC and lower specific surface areas (as shown in **Fig.3** panel (b) black dotted line). What's more, the organic coating of aerosol particles can largely reduce the reactivity of surface heterogeneous reactions (Zelenov et al., 2017; Anttila et al., 2006; Folkers et al., 2003; Ryder et al., 2015) and may cause the Mn-surface pathway less important. High mass concentrations of organic aerosol (OA) were observed in Beijing both in winter and summer (Hu et al., 2016), based on measured result (Yu et al., 2019a) from transmission electron microscopy, up to 74 % by a number of non-sea-salt sulfate particles were coated with organic matter (OM). The organic coating can effectively reduce the reactive sites in the surface of particles hence reduce the reaction probability of SO_2 with surface metal. In the other hand, the widespread presence of aerosol organic coating can also influence the bulk SO_2 catalysed by aqueous TMI but not only the surface reactions. This effect is mainly achieved by the change of SO_2 solubility and diffusion coefficient rather than the rates of catalytic reactions with TMI. Although the solubility of SO_2 in organic solvent changes a lot with the component of organic (Zhang et al., 2013; Huang et al., 2014a), according to previous studies of SO_2 uptake coefficient with sea-salt aerosol (Gebel et al., 2000) and secondary organic aerosol (SOA) (Yao et al., 2019), no obvious uptake coefficient reduction was observed with the organic coating further proving the minor influence of the organic coating on bulk reaction rates. The catalytic reaction of SO_2 with aqTMI may less affected by aerosol organic coating compared to SO_2 with Mn-surface. For these reasons, the surface reaction of SO_2 with Mn and other metals in actual aerosol conditions

remain unclear with high uncertainties and need further evaluation. The relevant calculation results of WD-14 and PKU-17 in this paper represent the upper limit of Mn-surface contribution. The missing contribution in WD-14 polluted conditions may mainly come from organic photosensitizing molecules such as HULIS (Wang et al., 2020) under stronger UV in summer or other SOA coupled mechanisms.

The results in this paper indicate that sulfate formation has different chemical behaviours in different conditions. Aqueous TMI-catalysed oxidation was the most important pathway followed by the surface oxidation of Mn in both winter and summer, while the hydroxyl and criegee radicals oxidations contribute significantly in summer. Due to the differences in the physical and chemical properties between aerosol water, fog water and cloud, nitrogen dioxide oxidation is the dominant pathway in higher pH range and hydroperoxide and ozone oxidations dominated for the cloud. In model studies, the averaged and fixed values should be used dialectically and carefully in the calculation of sulfate formation rate because of the mutual restriction between factors such as pH, effective ion activity and concentration, and aerosol water content. Model evaluation or numerical calculations of secondary pollutants should focus on the application of actual atmospheric conditions observed in field campaigns with the application of closure study. Our results highlight the important role of aerosol aqTMI in sulfate formation during haze periods and the monitoring network of aerosol metal is necessary for the studies of secondary sulfate formation. The aqTMI independent of solar radiation also explains the explosive growth of sulfate production at night-time, which is frequently observed during haze episodes in the NCP.

Compared to the gas-phase oxidants, the control of anthropogenic emissions of aerosol TMI is conducive to the reduction of secondary sulfates. The promotion of clean energy strategies aiming

at reducing coal burning and vehicle emissions to improve air quality in North China has reduced not only the primary emissions of SO_2 but also the anthropogenic emissions of aerosol TMIs (Liu et al., 2018) and thus the production of secondary sulfate. What' more, China's ecological and environmental protection measures for tree planting and afforestation are conducive to reducing the generation of dust especially in the spring can further reducing the quality of metal Fe concentrations in aerosols.

Our findings showed that urban aerosol TMIs contribute to sulfate formation during haze episodes and play a key role in developing mitigation strategies and public health measures in megacities worldwide, but the physicochemical processes of transition metals in particles require further research. Dissolved Mn concentrations in this study were estimated based on previous studies. The solubility of transition metals in aerosol water varying largely due to several factors including various source emissions, aerosol organic matter and pH (Paris and Desboeufs, 2013; Wozniak et al., 2015; Tapparo et al., 2020) were not fully considered in this study. Influences of organic matter and photosensitizing molecules on the solubility of transition metal and the mechanism of sulfate formation need further research to understand this complex and dynamic multiphase process from a broader perspective.

Methods

M. 1 Sampling location and experimental methods

The data from the 2014 Wangdu (WD) and 2017 Peking University (PKU) field campaigns, both conducted in summer, were used in our analysis. The WD field campaign was carried out from June to July 2014 at a rural site in Hebei (38.70° N, 115.15° E) characterized by severe photochemical

smog pollution (Tan et al., 2017; Song et al., 2020). The 2017 PKU campaign was performed from November to December 2017 at the campus of Peking University (39.99° N, 116.31° E), which is in the city centre of Beijing and characterized by strong local anthropogenic emissions from two major roads (Ma et al., 2019).

Observations from both field campaigns include gas-phase measurements of SO_2 and O_3 from commercial Thermo Scientific monitors and NO_2 detected after conversion through a custom-built photolytic converter with UV-LED at 395 nm; aerosol number concentration and distribution from a set of commercial particle instruments containing Nano scanning mobility particle sizer (SMPS) and aerodynamic particle sizer (APS) to cover the size range of 3 nm to 10 μm. The mass concentration of $PM_{2.5}$ was measured by commercial Ambient Particulate Monitor (TEOM). The In-situ Gas and Aerosol Compositions monitor (IGAC) (Young et al., 2016), which can collect gases and p articles simultaneously, was used to measure water-soluble ions online with 1-h time resolution. Both gas and aerosol samples were injected into 10 mL glass syringes, which were connected to an ion chromatograph (IC) for analysis (30-min time resolution for each sample). The concentrations of eight water soluble inorganic ions (NH_4^+, Na^+, K^+, Ca^{2+}, Mg^{2+}, SO_4^{2-}, NO_3^-, and Cl^-) in fine particles were measured. Transition metal (Fe and Cu) concentrations in $PM_{2.5}$ were measured using the Xact 625 Ambient Metal Monitor. With Xact, ambient air was introduced through a $PM_{2.5}$ cyclone inlet at a constant flow rate of 16.7 L min^{-1} and collected on the reel-to-reel poly tetrafluoroethylene filter. Then trace elements in ambient fine particles on the filter were automatically detected using the United States Environmental Protection Agency (USEPA) standard method via x-ray fluorescence (XRF) analysis (Gao et al., 2016; Zhang et al., 2019). Ambient temperature and pressure data were measured using commercial meteorological sensors; selected

volatile organic compounds (VOCs) were measured via off-line gas chromatography–mass spectrometry (GC-MS) in tower measurements using sampling canisters and via online GC−MS in the surface campaign. The OH and HO_2 concentrations were measured via laser-induced fluorescence (LIF) with the time resolution of 30 s as described in previous study (Ma et al., 2019). The concentrations of gas-phase peroxides were measured using high-performance liquid chromatography (HPLC, Agilent 1200, USA) with a time resolution of 21 min.

M. 2 Brief overview of the PKU-MARK model

The Multiple-phAse Reaction Kinetic Model (PKU-MARK) was first developed to calculate the heterogeneous reaction rate of reactive gas molecules (Song et al., 2020). The units of aqueous reagents are converted to molecules·cm^{-3} in the model by a factor k_{mt}, which combines both gas-phase molecular diffusion and liquid-phase interface mass transport processes (Schwartz, 1984; Schwartz, 1986) and used in the calculation for gas–liquid multiphase reactions in many modelling studies (Lelieveld and Crutzen, 1991; Chameides and Stelson, 1992a; Sander, 1999; Hanson et al., 1994; Song et al., 2020). In this study, the PKU-MARK model was further developed with the correction of ionic strength for all ions and reactants and applied to a size-segregated system to investigate the influence of aerosol particle size distribution and ALWC distribution. Eleven bins of aerosol particle diameters and corresponding ALWC values were applied in the model. With the input of one-hour averaged parameters observed in the field campaign, the PKU-MARK model produced the state-state concentrations of aqueous reactants including reactive oxygen species (H_2O_2, O_3, OH, HO_2, O_2^-), Fe (III), Mn (II), $SO_{2(aq)}$, and $NO_{2(aq)}$. Considering the mutual influence of various factors in the reaction system can effectively prevent bias caused by arbitrarily fixing a certain value as was often done in previous studies.

M. 3 Calculation of aerosol pH, aerosol liquid water, and ionic strength

ALWC and aerosol pH were calculated using the ISORROPIA-II model and measured concentrations of inorganic ions in particles. ISORROPIA-II is a thermodynamic equilibrium model that predicts the physical state and composition of atmospheric inorganic aerosols. Its ability to predict pH has been demonstrated in detail in previous studies (Guo et al., 2015; Xu et al., 2015). Ionic strength was calculated via equation (2) (Ross and Noone, 1991):

$$I_s = \frac{1}{2} \cdot \sum m_i \cdot z_i^2, \quad (2)$$

where m_i is the molality of an ion (mol L^{-1}), and z_i is the corresponding charge. In the PKU-MARK model, reaction rates were replaced by the activity coefficient. The ionic strength was estimated using the ISORROPIA-II model assuming that the condensed phase is in the meta-stable state and complete external mixing state.

In order to consider the influence of particle diameter on aqueous SO_2 concentrations, which is key to calculate sulfate formation, we used a 11-bin actual particle diameter distribution rather than one even distribution used in previous studies (Cheng et al., 2016). The distribution of particle number concentration and water content is illustrated in **Fig. S2**. We also considered the distribution of ALWC in different particle diameter bins based on the κ–Köhler theory (Petters and Kreidenweis, 2007) using observed kappa values from High Humidity Tandem Differential Mobility Analyser (HH-TDMA) and the Twin Differential Mobility Particle Sizer (TDMPS)/APS (Bian et al., 2014). Calculated ALWC values were strongly correlated with the ISORROPIA-II results (**Fig. S3)**.

To combine both gas-phase molecular diffusion and liquid-phase interface mass transport processes, the approach adopted in this study uses one variable called k_{mt} (Schwartz, 1984; Schwartz, 1986), which is used in multiphase reactions in many modelling studies (Lelieveld and Crutzen, 1991;

Chameides and Stelson, 1992b; Sander, 1999; Hanson et al., 1994). The definition of k_{mt} is given in equation (3):

$$k_{mt} = (\frac{{R_d}^2}{3D_g} + \frac{4R_d}{3v_{HO_2}\alpha})^{-1}. \quad (3)$$

The rate of gas-phase reactions (*X*) diffusing and dissolving to the condensed phase can be calculated in the framework of aqueous-phase reactions as $k_{mt\_X} \times ALWC$ where *X* is the reactant molecule (please see **Table S8** for more details). Moreover, the conversion rate of aqueous-phase reactions to gas-phase reactions can be calculated as $\frac{k_{mt\_X}}{H^{cc} \times RT}$. The unit of k_{mt} is s^{-1}, as k_{mt} contains the conversion from m_{air}^{-3} of the gas-phase molecule concentrations to m_{aq}^{-3} of the aqueous-phase molecule concentrations. Particle diameter can influence the mass transport rate of SO_2 and its aqueous concentration. Based on the model results of (Xue et al., 2016), diameter had an impact on sulfate formation rates: for larger particles (radius >1 μm), k_{mt} is determined by gas-phase diffusion; for smaller particles (radius <1 μm), k_{mt} is determined by the accommodation process. The PKU-MARK model can simultaneously simulate two-phase (gas and liquid) reaction systems in the same framework.

M. 4 Model Evaluation

Concentrations of sulfate were calculated by integrating an extension of the Eulerian box model described in previous study (Seinfeld and Pandis, 2016). Sulfate concentrations are related to dry deposition, transport, dilution as the boundary layer height (BLH) expands, emissions, and net production. Due to the higher and more dramatically diurnal changing BLH in summer (Lou et al., 2019), and the lack of relevant data in WD-14 field campaign, we could not get the modelled results of sulfate concentrations in summer haze periods. Direct emissions and transport of sulfate were not considered in the calculation because secondary sulfate is the predominant source in winter haze

periods. Dilution was not considered either because the atmosphere is relatively homogeneous during winter haze episodes. Since haze events are normally accompanied by a low boundary layer height (H_t), H_t was set at 300 m at night-time and 450 m at noon (Xue et al., 2016). At other times, H_t was estimated using a polynomial (n = 2) regression as recommended in previous study (Xue et al., 2016). The diurnal trends of sulfate concentrations of the winter haze period using the deposition velocity of 1.5 cm/s and of 2 cm/s in summer are shown in **Fig. 1 (c) and (d)**. Model results had the same trend with the observed values and could explain the missing source of sulfate aerosol to some extent in winter while with high uncertainties in summer condition.

Table 1. Averaged results of observed meteorological parameters, trace gases concentrations transition metal concentrations such as Fe, Cu, Mn and calculated ALWC, ionic strength, pH and sulfate formation rates in different pollution conditions in two field campaigns (±1σ).

Parameters	Clean	Slightly polluted	Polluted	Highly polluted
Winter				
RH (%)	25.0±8.3	37.1±11.5	44.8±11.9	63.6±19.5
Temperature (K)	273.0±4.6	274.1±3.3	273.6±2.6	273.8±2.3
SO_2 (ppbV)	2.4±1.4	5.8±2.0	6.5±2.6	5.5±3.0
NO_2 (ppbV)	21.1±10.4	37.6±6.3	44.1±6.1	57.6±8.7
OH (#/cm^3)	(4.67±3.73)×10^5	(5.02±5.22)×10^5	(4.42±2.78)×10^5	(4.36±3.06)×10
H_2O_2 (pptV)	29.8±20.8	23.5±27.2	19.5±39.6	20.9±22.8
O_3 (ppbV)	14.8±11.9	3.2±5.7	2.1±2.7	1.1±1.2
SO_4^{2-} (μg/m^3)	3.5±1.5	6.4±3.5	8.3±4.2	16.6±6.6
Fe (ng/m^3)	348.4±263.0	564.2±188.2	725.5±258.6	1300.6±289.5
Cu (ng/m^3)	7.0±5.0	13.8±4.2	18.7±6.0	29.3±6.6
Mn (ng/m^3)	12.4±9.4	20.1±6.7	25.9±9.2	46.5±10.3
ALWC (μg/m^3)	3.1±2.6	3.8±4.4	11.9±15.6	82.4±67.3
Surface area (μm^2/cm^3)	263.2±171.5	714.3±242.2	1253.3±448.9	2628.6±1164.4
$PM_{2.5}$ (μg/m^3)	18.3±10.1	52.0±10.0	101.7±18.2	190.0±30.0
pH	4.43±1.12	4.52±0.76	4.93±0.57	4.77±0.39
Ionic Strength (M)	170.34±88.32	89.32±55.19	61.59±38.7	36.27±36.93
d[S(VI)]/dt (μg/m^3/h)	1.3±1.88	2.25±2.15	2.35±2.19	3.98±2.75
Summer				
RH (%)	69.5±17.9	64.4±18.4	66.4±13.0	65.6±7.7

Temperature (K)	296.5±3.6	298.5±4.4	299.1±2.9	298.9±3.1
SO_2 (ppbV)	2.4±2.0	4.6±4.4	5.6±5.0	7.9±4.0
NO_2 (ppbV)	8.7±4.9	9.6±5.6	9.0±5.5	12.3±6.1
OH (#/cm^3)	(2.38±2.44)×10^5	(3.27±3.21)×10^5	(2.77±2.26)×10^5	(3.50±3.38)×10
H_2O_2 (pptV)	466.2±571.6	355.5±488.0	596.1±777.0	173.6±348.6
O_3 (ppbV)	46.0±30.3	50.9±30.6	53.0±26.6	48.5±28.5
SO_2^{4-} (μg/m^3)	7.2±2.6	11.0±4.9	17.8±6.0	24.4±6.0
Fe (ng/m^3)	521.6±286.6	469.3±151.7	535.2±177.0	730.9±156.6
Cu (ng/m^3)	26.6±18.8	37.7±31.8	33.8±26.0	47.1±36.3
Mn (ng/m^3)	18.6±10.2	16.8±5.4	19.1±6.3	26.1±5.6
ALWC (μg/m^3)	31.8±30.9	35.7±32.8	48.6±31.4	58.8±14.4
Surface area (μm^2/cm^3)	767.8±265.6	925.0±213.9	1389.0±312.6	1711.1±729.6
$PM_{2.5}$ (μg/m^3)	20.1±10.2	54.9±11.7	104.8±20.5	194.6±32.9
pH	4.48±0.48	4.19±0.66	4.17±0.48	4.33±0.44
Ionic Strength (M)	20.04±17.53	25.44±20.83	24.27±14.06	24.2±9.19
d[S(VI)]/dt (μg/m^3/h)	2.13±2.03	3.81±4.22	3.79±5.66	5.6±4.45

The concentration of Mn was estimated based on the ratio of Fe/Mn observed in urban Beijing in the literatures (summarized in **Table S9**). **All mentioned aerosol data is particle matters diameter smaller than 2.5 μm,and $PM_{2.5}$ refers to the dry mass concentration of fine particulate matters.**

Figure 1. Three-hour average sulfate formation rates during haze periods in winter and summer (a)&(b), corresponding effective Fe (III) concentrations and sulfate concentrations (c)&(d), sulfate formation rates (the histogram) and SOR (the dotted lines) in different pollution levels in two field campaigns (e)&(f).

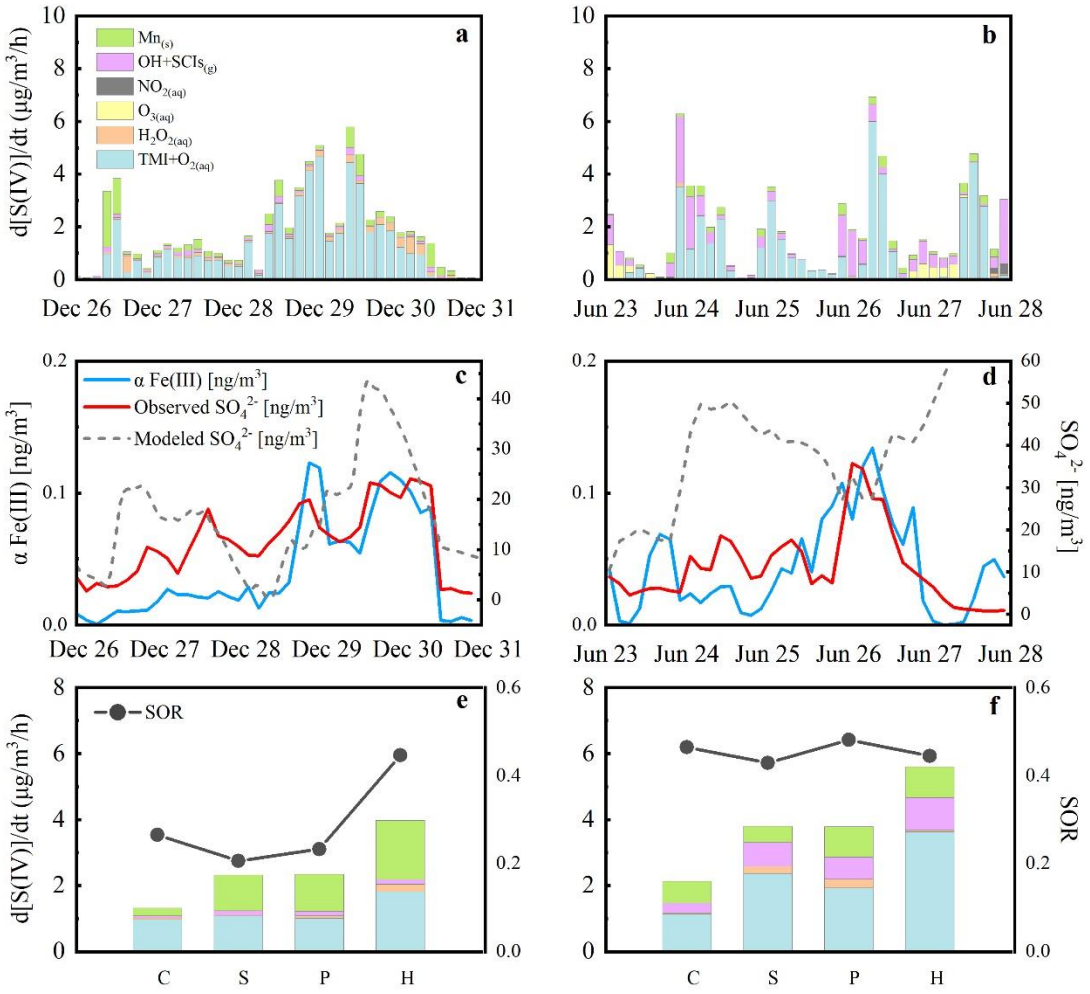

The contributions to sulfate formation from each multiphase oxidant pathways including Mn-surface oxidant (green), gas phase OH radical and Stabilized Criegee Intermediates (SCIs) oxidant (pink), aqueous phase NO_2 (grey), O_3 (yellow), H_2O_2 (orange) and aqTMI (blue) were colored in the figure. Obvious particle growth and removal was observed in winter (26th to 31st, December, 2017) and diurnal variation patterns of sulfate concentration were observed in summer (23th to 28th, June, 2014). Diurnal trends of modelled winter period's sulfate concentration (grey dash line) using deposition velocity as 1.5 cm/s in winter and 2 cm/s in summer are illustrated in panel (c) and (d). The dotted lines in the (e), winter and (f), summer

indicate the SOR with pollution level in the whole campaigns and the capitalized letters “C”, “S”, “P”, “H” are the abbreviations for “Clean”, “Slightly polluted”, “Polluted” and “highly polluted”, respectively.

Figure 2. Multiphase sulfate production under actual ambient conditions (a,c) and averaged conditions (b,d) in winter (a, b) and summer (c, d) in the North China Plain.

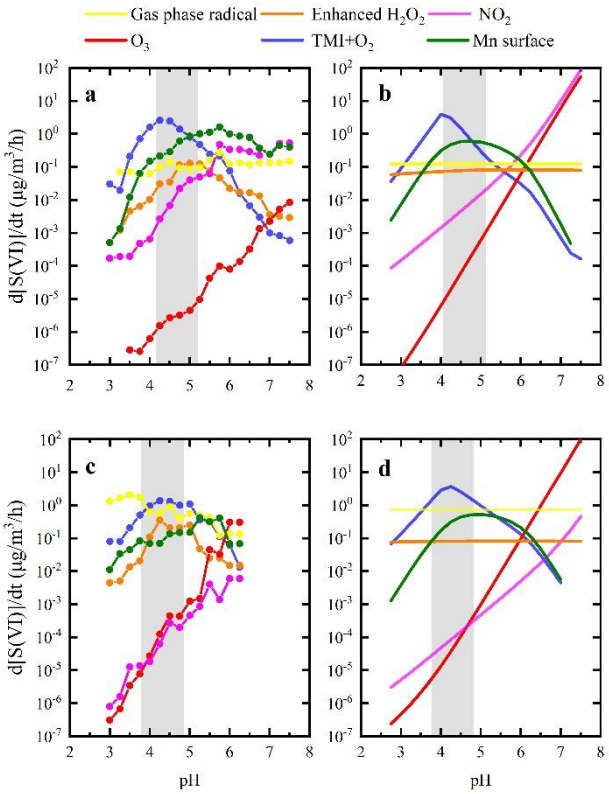

Given the actual measured concentration, the steady-state concentration of each reactant was calculated using the MARK model accounting for the impact of ionic strength on the Henry’s law coefficient of the gas-phase reactants. Panels (a) and (c) show the cluster averaged results with a pH span of 0.5. Panels (b) and (d) show the sulfate formation rate obtained by fixing the average precursors levels during the haze periods and by changing the aerosol pH, which is consistent with the calculation method of previous studies (Cheng et al., 2016). Grey-shaded areas indicate the ISORROPIA-II (Fountoukis and Nenes, 2007) model calculated pH

ranges during the haze periods of two field campaigns. The coloured solid lines represent sulfate production rates calculated for different multiphase reaction pathways with oxidants: enhanced H_2O_2, O_3, TMIs, NO_2, surface Mn and gas-phase radicals (OH+SCIs). The solid orange line represents the calculated sulfate formation rate via H2O2 with a factor of 100 in winter and summer according to the latest research results (Liu et al., 2020b). Reactant concentrations, aqueous reaction rate expressions, and rate coefficients are summarized in the SI.

Figure 3. Variation of $PM_{2.5}$, ionic strength, aerosol pH, particle specific surface areas and sulfate formation rates from different pathways with aerosol liquid water content (ALWC) during winter field campaign.

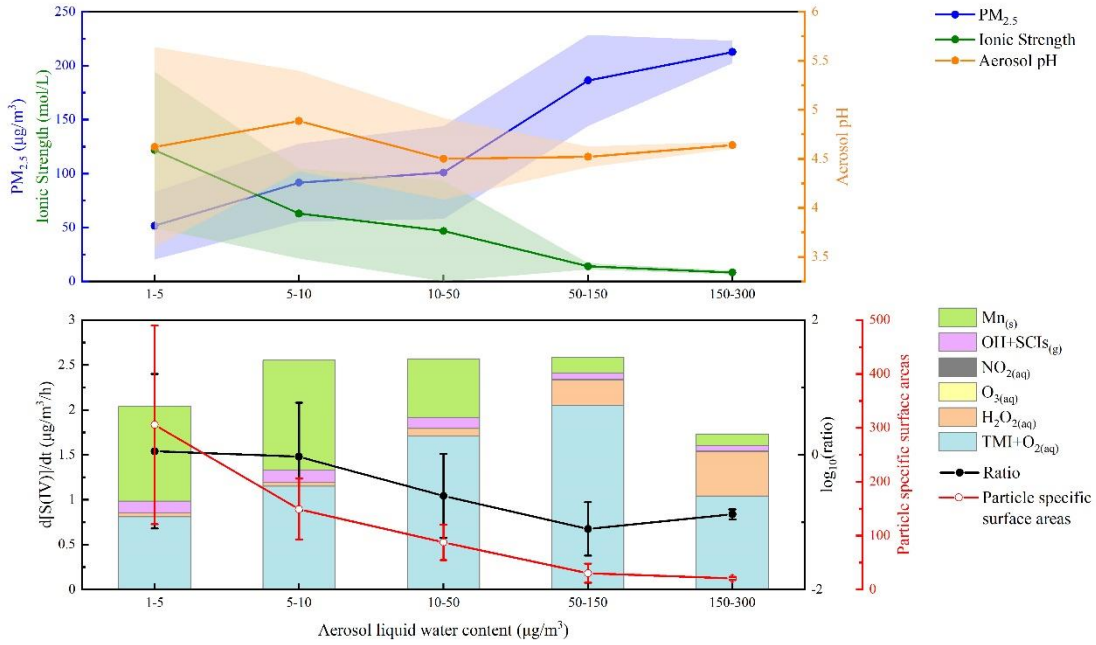

The total number of valid data points shown in the figure is 479. The shaded area refer to the error bar (±1 σ) of $PM_{2.5}$ mass concentration, aerosol ionic strength and pH calculated by ISORROPIA-II(Fountoukis and Nenes, 2007). Ratio in the second panel refers to the ratio of

contributions from Mn-surface to aqTMI to produce sulfate. Particle specific surface areas represent the ratio of particle surface area ($\mu m^2/cm^3$) and mass concentration ($\mu g/m^3$).

Figure 4. Bar graph showing modelled contributions of various pathways to sulfate formation under different pollution conditions.

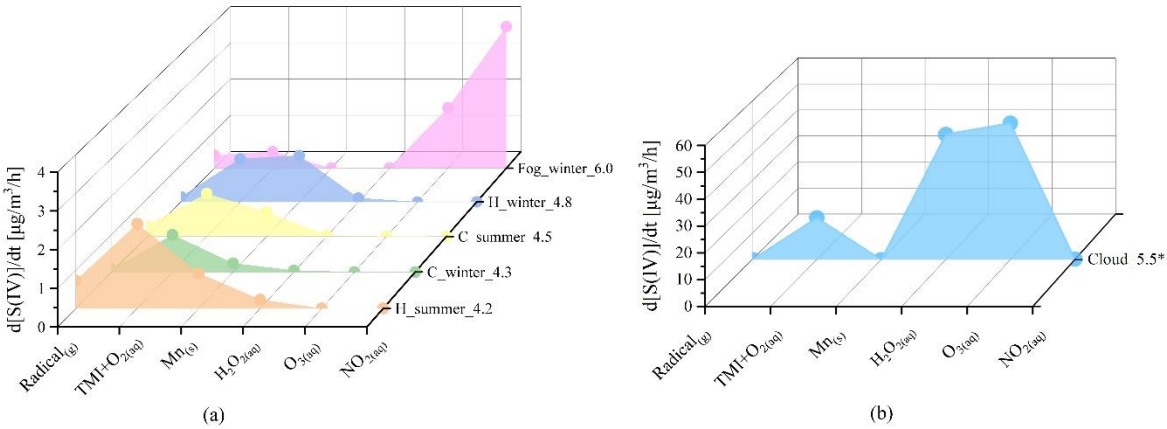

Different pollution conditions including clear ($PM_{2.5}$ smaller than 35 μg/m^3) in winter PKU 2017 (C_winter_4.3) and summer WD 2014 (C_summer_4.5); pollution ($PM_{2.5}$ larger than 75 μg/m^3) in PKU 2017 (H_winter_4.8), WD 2014 (H_summer_4.2); fog conditions used in a previous study (Xue et al., 2016) (Fog_winter_6.0) and cloud conditions (Cloud_5.5) simulated by Seinfeld and Pandis (2016). The number in each label indicates the average pH value chosen in these calculations. We assumed that the cloud water content is 0.1 g/m^3 in the last condition, and reduced the H_2O_2 concentration to 0.1 ppb compared to the high value used before (Seinfeld and Pandis, 2016).

Data Availability

Data supporting this publication are available upon request for the corresponding author (k.lu@pku.edu.cn).

Conflict of interests

The authors declare that they have no conflict of interest.

Acknowledgements

This study was supported by the by the National Key Research and Development Program of China (2019YFC0214800), the Beijing Municipal Natural Science Foundation for Distinguished Young Scholars (JQ19031), the National Key Research Program for Air Pollution Control (DQGG202002), the National Natural Science Foundation of China (21976006).

Author Contributions

Keding Lu conceived the study. Huan Song and Keding Lu developed the MARK model for multiphase simulations. Can Ye provide supports in the calculation. Huan Song performed the model simulations and wrote the manuscript with Keding Lu and Can Ye. Keding Lu and Yuanhang Zhang lead the two field campaigns. Keding Lu, Huabin Dong, Shule Li, Shiyi Chen, Zhijun Wu, Mei Zheng, Limin Zeng, Min Hu & Yuanhang Zhang provide campaign data for the analysis.

Supplementary Information

Supplementary information includes:

- Supplementary Information Text

  Text S1. Activity coefficients of main reactants in the MARK model

Text S2. The concentration of aerosol particle transition metals in urban areas

- Supplementary Information Figures Fig.S1-S9

Fig. S1. Ionic strength of aerosol particle solution influence on the aqTMI rate constant.

Fig. S2. Distribution of ALWC and number concentration with aerosol particle bins in two campaigns.

Fig. S3. Calculated aerosol water by ISORROPIA-II model and H-TDMA method in two field campaigns during haze periods. The plots were coloured with the relative humidity values. The black dashed line in the figure is the 1:1 baseline, and the red solid line is the linear fitting result assuming the intercept is zero.

Fig. S4. Time series of observed gas-phase pollutants concentrations, RH, Temperature, PM2.5 mass loading and calculated aerosol pH and water content and sulfate formation rates in these four haze periods in PKU-17 field campaign.

Fig. S5. SOR ($\equiv n(SO_2)/n(SO_2+SO_4^{2-})$) correlations with effective Fe (III) concentrations in PKU-17 winter field campaign.

Fig. S6. SOR ($\equiv n(SO_2)/n(SO_2+SO_4^{2-})$)correlations with odd oxygen ($[O_x] \equiv [O_3]+[NO_2]$) and relative humidity (RH) in WD-14 summer field campaign

Fig. S7 The “dilution effect” of Fe mass concentration and ALWC increasing with PM mass in winter and summer.

Fig. S8. Variation of PM2.5, ionic strength, aerosol pH, particle specific surface areas and sulfate formation rates from different pathways with aerosol liquid water content (ALWC) during summer field campaign.

- Supplementary Information Tables S1-S9.

References

Alexander, B., Park, R. J., Jacob, D. J., and Gong, S.: Transition metal-catalyzed oxidation of atmospheric sulfur: Global implications for the sulfur budget, Journal of Geophysical Research: Atmospheres, 114, https://doi.org/10.1029/2008JD010486, 2009.

Anttila, T., Kiendler-Scharr, A., Tillmann, R., and Mentel, T. F.: On the Reactive Uptake of Gaseous Compounds by Organic-Coated Aqueous Aerosols: Theoretical Analysis and Application to the Heterogeneous Hydrolysis of N2O5, The Journal of Physical Chemistry A, 110, 10435-10443, 10.1021/jp062403c, 2006.

Atkinson, R., Baulch, D. L., Cox, R. A., Crowley, J. N., Hampson, R. F., Hynes, R. G., Jenkin, M. E., Rossi, M. J., and Troe, J.: Evaluated kinetic and photochemical data for atmospheric chemistry: Volume I - gas phase reactions of Ox, HOx, NOx and SOx species, Atmospheric Chemistry and Physics, 4, 1461-1738, 2004.

Baker, A. R. and Jickells, T. D.: Mineral particle size as a control on aerosol iron solubility, Geophysical Research Letters, 33, 10.1029/2006gl026557, 2006.

Baker, A. R., Jickells, T. D., Witt, M., and Linge, K. L.: Trends in the solubility of iron, aluminium, manganese and phosphorus in aerosol collected over the Atlantic Ocean, Marine Chemistry, 98, 43-58, 10.1016/j.marchem.2005.06.004, 2006.

Barth, M. C., Hess, P. G., and Madronich, S.: Effect of marine boundary layer clouds on tropospheric chemistry as analyzed in a regional chemistry transport model, Journal of Geophysical Research: Atmospheres, 107, AAC 7-1-AAC 7-12, https://doi.org/10.1029/2001JD000468, 2002.

Bian, Y. X., Zhao, C. S., Ma, N., Chen, J., and Xu, W. Y.: A study of aerosol liquid water content based on hygroscopicity measurements at high relative humidity in the North China Plain, Atmospheric Chemistry and Physics, 14, 6417-6426, 10.5194/acp-14-6417-2014, 2014.

Chameides, W. and Stelson, A.: Aqueous-phase chemical processes in deliquescent sea-salt aerosols: A mechanism that couples the atmospheric cycles of S and sea salt, Journal of Geophysical Research: Atmospheres, 97, 20565-20580, 1992a.

Chameides, W. L. and Stelson, A. W.: Aqueous-phase chemical processes in deliquescent seasalt aerosols, Ber Bunsen Phys Chem, 96, 461-470, 1992b.

Cheng, Y., Zheng, G., Wei, C., Mu, Q., Zheng, B., Wang, Z., Gao, M., Zhang, Q., He, K., Carmichael, G., Pöschl, U., and Su, H.: Reactive nitrogen chemistry in aerosol water as a source of sulfate during haze events in China, Science Advances, 2, e1601530, 10.1126/sciadv.1601530, 2016.

Duan, J. C., Tan, J. H., Wang, S. L., Hao, J. M., and Chail, F. H.: Size distributions and sources of elements in particulate matter at curbside, urban and rural sites in Beijing, Journal of Environmental Sciences, 24, 87-94, 10.1016/s1001-0742(11)60731-6, 2012.

Fang, T., Guo, H., Zeng, L., Verma, V., Nenes, A., and Weber, R. J.: Highly Acidic Ambient Particles, Soluble Metals, and Oxidative Potential: A Link between Sulfate and Aerosol Toxicity, Environ. Sci. Technol., 51, 2611-2620, 10.1021/acs.est.6b06151, 2017.

Folkers, M., Mentel, T. F., and Wahner, A.: Influence of an organic coating on the reactivity of aqueous aerosols probed by the heterogeneous hydrolysis of N2O5, Geophysical Research Letters, 30, https://doi.org/10.1029/2003GL017168, 2003.

Fountoukis, C. and Nenes, A.: ISORROPIA II: a computationally efficient thermodynamic equilibrium model for K^+-Ca^{2+}-Mg^{2+}-NH_4^+-Na^+-SO_4^{2-}-NO_3^--Cl^--H2O aerosols, Atmospheric Chemistry and Physics Discussions, 7, 1893-1939, 2007.

Gao, J., Peng, X., Chen, G., Xu, J., Shi, G.-L., Zhang, Y.-C., and Feng, Y.-C.: Insights into the chemical characterization and sources of $PM_{2.5}$ in Beijing at a 1-h time resolution, Sci. Total Environ., 542, 162-171, 2016.

Gebel, M. E., Finlayson-Pitts, B. J., and Ganske, J. A.: The uptake of SO2 on synthetic sea salt and some of its components, Geophysical Research Letters, 27, 887-890, https://doi.org/10.1029/1999GL011152, 2000.

Goliff, W. S. and Stockwell, W. R.: The regional atmospheric chemistry mechanism, version 2, an update, International con-ference on Atmospheric Chemical Mechanisms, University of California, Davis, 96, 36, 2008.

Goliff, W. S., Stockwell, W. R., and Lawson, C. V.: The regional atmospheric chemistry mechanism, version 2, Atmos. Environ., 68, 174-185, 2013.

Guo, H., Weber, R. J., and Nenes, A.: High levels of ammonia do not raise fine particle pH sufficiently to yield nitrogen oxide-dominated sulfate production, Sci Rep-Uk, 7, 12109, 10.1038/s41598-017-11704-0, 2017.

Guo, H., Xu, L., Bougiatioti, A., Cerully, K. M., Capps, S. L., Hite, J. R., Carlton, A. G., Lee, S. H., Bergin, M. H., Ng, N. L., Nenes, A., and Weber, R. J.: Fine-particle water and pH in the southeastern United States, Atmospheric Chemistry and Physics, 15, 5211-5228, 10.5194/acp-15-5211-2015, 2015.

Guo, S., Hu, M., Zamora, M. L., Peng, J. F., Shang, D. J., Zheng, J., Du, Z. F., Wu, Z., Shao, M., Zeng, L. M., Molina, M. J., and Zhang, R. Y.: Elucidating severe urban haze formation in China, Proceedings of the National Academy of Sciences of the United States of America, 111, 17373-17378, 10.1073/pnas.1419604111, 2014.

Hanson, D. R., Ravishankara, A. R., and Solomon, S.: Heterogeneous reactions in sulfuric-acid aerosol: A framework for model calculations, J. Geophys. Res.-Atmos., 99, 3615-3629, 10.1029/93jd02932, 1994.

He, P., Alexander, B., Geng, L., Chi, X., Fan, S., Zhan, H., Kang, H., Zheng, G., Cheng, Y., and Su, H.: Isotopic constraints on heterogeneous sulfate production in Beijing haze, Atmospheric Chemistry and Physics, 18, 5515-5528, 2018.

Heal, M. R., Hibbs, L. R., Agius, R. M., and Beverland, L. J.: Total and water-soluble trace metal content of urban background PM_{10}, $PM_{2.5}$ and black smoke in Edinburgh, UK, Atmos. Environ., 39, 1417-1430, 10.1016/j.atmosphere.2004.11.026, 2005.

Hsu, S.-C., Wong, G. T. F., Gong, G.-C., Shiah, F.-K., Huang, Y.-T., Kao, S.-J., Tsai, F., Candice Lung, S.-C., Lin, F.-J., Lin, I. I., Hung, C.-C., and Tseng, C.-M.: Sources, solubility, and dry deposition of aerosol trace elements over the East China Sea, Marine Chemistry, 120, 116-127, https://doi.org/10.1016/j.marchem.2008.10.003, 2010.

Hu, W., Hu, M., Hu, W., Jimenez, J. L., Yuan, B., Chen, W., Wang, M., Wu, Y., Chen, C., Wang, Z., Peng, J., Zeng, L., and Shao, M.: Chemical composition, sources, and aging process of submicron aerosols in Beijing: Contrast between summer and winter, Journal of Geophysical Research: Atmospheres, 121, 1955-1977, https://doi.org/10.1002/2015JD024020, 2016.

Huang, K., Xia, S., Zhang, X.-M., Chen, Y.-L., Wu, Y.-T., and Hu, X.-B.: Comparative Study of the Solubilities of SO2 in Five Low Volatile Organic Solvents (Sulfolane, Ethylene Glycol, Propylene Carbonate, N-Methylimidazole, and N-Methylpyrrolidone), Journal of Chemical & Engineering Data, 59, 1202-1212, 10.1021/je4007713, 2014a.

Huang, R.-J., Zhang, Y., Bozzetti, C., Ho, K.-F., Cao, J.-J., Han, Y., Daellenbach, K. R., Slowik, J. G., Platt, S. M., Canonaco, F., Zotter, P., Wolf, R., Pieber, S. M., Bruns, E. A., Crippa, M., Ciarelli, G.,

Piazzalunga, A., Schwikowski, M., Abbaszade, G., Schnelle-Kreis, J., Zimmermann, R., An, Z., Szidat, S., Baltensperger, U., Haddad, I. E., and Prévôt, A. S. H.: High secondary aerosol contribution to particulate pollution during haze events in China, Nature, 514, 218-222, 10.1038/nature13774, 2014b.

Huang, X., Song, Y., Zhao, C., Li, M., Zhu, T., Zhang, Q., and Zhang, X.: Pathways of sulfate enhancement by natural and anthropogenic mineral aerosols in China, Journal of Geophysical Research: Atmospheres, 119, 14,165-114,179, https://doi.org/10.1002/2014JD022301, 2014c.

Ito, A., Myriokefalitakis, S., Kanakidou, M., Mahowald, N. M., Scanza, R. A., Hamilton, D. S., Baker, A. R., Jickells, T., Sarin, M., Bikkina, S., Gao, Y., Shelley, R. U., Buck, C. S., Landing, W. M., Bowie, A. R., Perron, M. M. G., Guieu, C., Meskhidze, N., Johnson, M. S., Feng, Y., Kok, J. F., Nenes, A., and Duce, R. A.: Pyrogenic iron: The missing link to high iron solubility in aerosols, Science Advances, 5, eaau7671, 10.1126/sciadv.aau7671, 2019.

Koop, T., Luo, B., Tsias, A., and Peter, T.: Water activity as the determinant for homogeneous ice nucleation in aqueous solutions, Nature, 406, 611-614, 2000.

Lelieveld, J. and Crutzen, P. J.: The role of clouds in tropospheric photochemistry, J Atmos Chem, 12, 229-267, 10.1007/bf00048075, 1991.

Li, J., Zhang, Y.-L., Cao, F., Zhang, W., Fan, M., Lee, X., and Michalski, G.: Stable Sulfur Isotopes Revealed a Major Role of Transition-Metal Ion-Catalyzed SO_2 Oxidation in Haze Episodes, Environ. Sci. Technol., 54, 2626-2634, 10.1021/acs.est.9b07150, 2020a.

Li, J., Zhu, C., Chen, H., Fu, H., Xiao, H., Wang, X., Herrmann, H., and Chen, J.: A More Important Role for the Ozone-S(IV) Oxidation Pathway Due to Decreasing Acidity in Clouds, Journal of Geophysical Research: Atmospheres, 125, e2020JD033220, https://doi.org/10.1029/2020JD033220, 2020b.

Li, L., Hoffmann, M. R., and Colussi, A. J.: Role of Nitrogen Dioxide in the Production of Sulfate during Chinese Haze-Aerosol Episodes, Environ. Sci. Technol., 52, 2686-2693, 10.1021/acs.est.7b05222, 2018.

Lippmann, M. and Thurston, G. D.: Sulfate concentrations as an indicator of ambient particulate matter air pollution for health risk evaluations, J Expo Anal Environ Epidemiol, 6, 123-146, 1996.

Liu, C., Ma, Q., Liu, Y., Ma, J., and He, H.: Synergistic reaction between SO_2 and NO_2 on mineral oxides: a potential formation pathway of sulfate aerosol, Physical Chemistry Chemical Physics, 14, 1668-1676, 10.1039/C1CP22217A, 2012.

Liu, J., Chen, Y., Chao, S., Cao, H., Zhang, A., and Yang, Y.: Emission control priority of $PM_{2.5}$-bound heavy metals in different seasons: A comprehensive analysis from health risk perspective, Sci. Total Environ., 644, 20-30, https://doi.org/10.1016/j.scitotenv.2018.06.226, 2018.

Liu, M., Song, Y., Zhou, T., Xu, Z., Yan, C., Zheng, M., Wu, Z., Hu, M., Wu, Y., and Zhu, T.: Fine particle pH during severe haze episodes in northern China, Geophysical Research Letters, 44, 5213-5221, https://doi.org/10.1002/2017GL073210, 2017.

Liu, P., Ye, C., Xue, C., Zhang, C., Mu, Y., and Sun, X.: Formation mechanisms of atmospheric nitrate and sulfate during the winter haze pollution periods in Beijing: gas-phase, heterogeneous and aqueous-phase chemistry, Atmospheric Chemistry and Physics, 20, 4153-4165, 2020a.

Liu, T., Clegg, S. L., and Abbatt, J. P. D.: Fast oxidation of sulfur dioxide by hydrogen peroxide in deliquesced aerosol particles, Proceedings of the National Academy of Sciences, 117, 1354-1359, 10.1073/pnas.1916401117, 2020b.

Lou, M., Guo, J., Wang, L., Xu, H., Chen, D., Miao, Y., Lv, Y., Li, Y., Guo, X., Ma, S., and Li, J.: On the

Relationship Between Aerosol and Boundary Layer Height in Summer in China Under Different Thermodynamic Conditions, Earth and Space Science, 6, 887-901, https://doi.org/10.1029/2019EA000620, 2019.
Ma, T., Furutani, H., Duan, F., Kimoto, T., Jiang, J., Zhang, Q., Xu, X., Wang, Y., Gao, J., Geng, G., Li, M., Song, S., Ma, Y., Che, F., Wang, J., Zhu, L., Huang, T., Toyoda, M., and He, K.: Contribution of hydroxymethanesulfonate (HMS) to severe winter haze in the North China Plain, Atmos. Chem. Phys., 20, 5887-5897, 10.5194/acp-20-5887-2020, 2020.
Ma, X., Tan, Z., Lu, K., Yang, X., Liu, Y., Li, S., Li, X., Chen, S., Novelli, A., and Cho, C.: Winter photochemistry in Beijing: Observation and model simulation of OH and HO_2 radicals at an urban site, Sci. Total Environ., 685, 85-95, 2019.
Mahowald, N. M., Baker, A. R., Bergametti, G., Brooks, N., Duce, R. A., Jickells, T. D., Kubilay, N., Prospero, J. M., and Tegen, I.: Atmospheric global dust cycle and iron inputs to the ocean, Global Biogeochemical Cycles, 19, https://doi.org/10.1029/2004GB002402, 2005.
Moch, J. M., Dovrou, E., Mickley, L. J., Keutsch, F. N., Cheng, Y., Jacob, D. J., Jiang, J., Li, M., Munger, J. W., and Qiao, X.: Contribution of hydroxymethane sulfonate to ambient particulate matter: A potential explanation for high particulate sulfur during severe winter haze in Beijing, Geophysical Research Letters, 45, 11,969-911,979, 2018.
Oakes, M., Rastogi, N., Majestic, B. J., Shafer, M., Schauer, J. J., Edgerton, E. S., and Weber, R. J.: Characterization of soluble iron in urban aerosols using near-real time data, Journal of Geophysical Research: Atmospheres, 115, https://doi.org/10.1029/2009JD012532, 2010.
Petters, M. D. and Kreidenweis, S. M.: A single parameter representation of hygroscopic growth and cloud condensation nucleus activity, Atmos. Chem. Phys., 7, 1961-1971, 10.5194/acp-7-1961-2007, 2007.
Ross, H. B. and Noone, K. J.: A numerical investigation of the destruction of peroxy radical by cu ion catalyzed-reactions on atmospheric particles, J Atmos Chem, 12, 121-136, 10.1007/bf00115775, 1991.
Ryder, O. S., Campbell, N. R., Morris, H., Forestieri, S., Ruppel, M. J., Cappa, C., Tivanski, A., Prather, K., and Bertram, T. H.: Role of Organic Coatings in Regulating N2O5 Reactive Uptake to Sea Spray Aerosol, The Journal of Physical Chemistry A, 119, 11683-11692, 10.1021/acs.jpca.5b08892, 2015.
Sander, R.: Modeling atmospheric chemistry: Interactions between gas-phase species and liquid cloud/aerosol particles, Surveys in Geophysics, 20, 1-31, 1999.
Sarwar, G., J. Godowitch, K. Fahey, J. Xing, David-C Wong, Jeff Young, S. Roselle, AND R. Mathur: Examination of Sulfate production by CB05TU, RACM2 & RACM2 with SCI initiated SO_2,oxidation in the Northern Hemisphere, Presented at Presentation at the CMAS Conference,Chapel Hill, NC2013.
Schwartz, S. E.: Gas phase and aqueous phase chemistry of HO_2 in liquid water clouds, J. Geophys. Res.-Atmos., 89, 1589-1598, 10.1029/JD089iD07p11589, 1984.
Schwartz, S. E.: Mass-transport considerations pertinent to aqueous phase reactions of gases in liquid-water clouds, in: Chemistry of multiphase atmospheric systems, Springer, 415-471, 1986.
Seigneur, C. and Saxena, P.: A theoretical investigation of sulfate formation in clouds, Atmospheric Environment (1967), 22, 101-115, https://doi.org/10.1016/0004-6981(88)90303-4, 1988.
Seinfeld, J. H. and Pandis, S. N.: Atmospheric chemistry and physics: from air pollution to climate change, John Wiley & Sons2016.
Shang, D., Peng, J., Guo, S., Wu, Z., and Hu, M.: Secondary aerosol formation in winter haze over

the Beijing-Tianjin-Hebei Region, China, Frontiers of Environmental Science & Engineering, 15, 34, 10.1007/s11783-020-1326-x, 2020.
Shao, J., Chen, Q., Wang, Y., Lu, X., He, P., Sun, Y., Shah, V., Martin, R. V., Philip, S., Song, S., Zhao, Y., Xie, Z., Zhang, L., and Alexander, B.: Heterogeneous sulfate aerosol formation mechanisms during wintertime Chinese haze events: air quality model assessment using observations of sulfate oxygen isotopes in Beijing, Atmos. Chem. Phys., 19, 6107-6123, 10.5194/acp-19-6107-2019, 2019.
Shi, Q., Tao, Y., Krechmer, J. E., Heald, C. L., Murphy, J. G., Kroll, J. H., and Ye, Q.: Laboratory Investigation of Renoxification from the Photolysis of Inorganic Particulate Nitrate, Environ. Sci. Technol., 55, 854-861, 10.1021/acs.est.0c06049, 2021.
Shi, Z., Krom, M. D., Jickells, T. D., Bonneville, S., Carslaw, K. S., Mihalopoulos, N., Baker, A. R., and Benning, L. G.: Impacts on iron solubility in the mineral dust by processes in the source region and the atmosphere: A review, Aeolian Research, 5, 21-42, https://doi.org/10.1016/j.aeolia.2012.03.001, 2012.
Sholkovitz, E. R., Sedwick, P. N., Church, T. M., Baker, A. R., and Powell, C. F.: Fractional solubility of aerosol iron: Synthesis of a global-scale data set, Geochimica et Cosmochimica Acta, 89, 173-189, https://doi.org/10.1016/j.gca.2012.04.022, 2012.
Song, H., Chen, X., Lu, K., Zou, Q., Tan, Z., Fuchs, H., Wiedensohler, A., Zheng, M., Wahner, A., Kiendler-Scharr, A., and Zhang, Y.: Influence of aerosol copper on HO_2 uptake: A novel parameterized equation, Atmos. Chem. Phys. Discuss., 2020, 1-23, 10.5194/acp-2020-218, 2020.
Tan, Z. F., Fuchs, H., Lu, K. D., Hofzumahaus, A., Bohn, B., Broch, S., Dong, H. B., Gomm, S., Haseler, R., He, L. Y., Holland, F., Li, X., Liu, Y., Lu, S. H., Rohrer, F., Shao, M., Wang, B. L., Wang, M., Wu, Y. S., Zeng, L. M., Zhang, Y. S., Wahner, A., and Zhang, Y. H.: Radical chemistry at a rural site (Wangdu) in the North China Plain: observation and model calculations of OH, HO_2 and RO_2 radicals, Atmospheric Chemistry and Physics, 17, 663-690, 10.5194/acp-17-663-2017, 2017.
Wang, G., Zhang, R., Gomez, M. E., Yang, L., Zamora, M. L., Hu, M., Lin, Y., Peng, J., Guo, S., Meng, J., Li, J., Cheng, C., Hu, T., Ren, Y., Wang, Y., Gao, J., Cao, J., An, Z., Zhou, W., Li, G., Wang, J., Tian, P., Marrero-Ortiz, W., Secrest, J., Du, Z., Zheng, J., Shang, D., Zeng, L., Shao, M., Wang, W., Huang, Y., Wang, Y., Zhu, Y., Li, Y., Hu, J., Pan, B., Cai, L., Cheng, Y., Ji, Y., Zhang, F., Rosenfeld, D., Liss, P. S., Duce, R. A., Kolb, C. E., and Molina, M. J.: Persistent sulfate formation from London Fog to Chinese haze, Proceedings of the National Academy of Sciences of the United States of America, 113, 13630-13635, 10.1073/pnas.1616540113, 2016.
Wang, W., Liu, M., Wang, T., Song, Y., Zhou, L., Cao, J., Hu, J., Tang, G., Chen, Z., Li, Z., Xu, Z., Peng, C., Lian, C., Chen, Y., Pan, Y., Zhang, Y., Sun, Y., Li, W., Zhu, T., Tian, H., and Ge, M.: Sulfate formation is dominated by manganese-catalyzed oxidation of SO_2 on aerosol surfaces during haze events, Nature Communications, 12, 1993, 10.1038/s41467-021-22091-6, 2021.
Wang, X., Gemayel, R., Hayeck, N., Perrier, S., Charbonnel, N., Xu, C., Chen, H., Zhu, C., Zhang, L., Wang, L., Nizkorodov, S. A., Wang, X., Wang, Z., Wang, T., Mellouki, A., Riva, M., Chen, J., and George, C.: Atmospheric Photosensitization: A New Pathway for Sulfate Formation, Environ. Sci. Technol., 54, 3114-3120, 10.1021/acs.est.9b06347, 2020.
Weber, R. J., Guo, H., Russell, A. G., and Nenes, A.: High aerosol acidity despite declining atmospheric sulfate concentrations over the past 15 years, Nature Geoscience, 9, 282-285, 10.1038/ngeo2665, 2016.
Welz, O., Savee, J. D., Osborn, D. L., Vasu, S. S., Percival, C. J., Shallcross, D. E., and Taatjes, C. A.: Direct Kinetic Measurements of Criegee Intermediate (CH_2OO) Formed by Reaction of CH_2I with

O_2^-, Science, 335, 204-207, 10.1126/science.1213229, 2012.
Wong, J. P. S., Yang, Y., Fang, T., Mulholland, J. A., Russell, A. G., Ebelt, S., Nenes, A., and Weber, R. J.: Fine Particle Iron in Soils and Road Dust Is Modulated by Coal-Fired Power Plant Sulfur, Environ. Sci. Technol., 54, 7088-7096, 10.1021/acs.est.0c00483, 2020.
Xu, L., Guo, H., Boyd, C. M., Klein, M., Bougiatioti, A., Cerully, K. M., Hite, J. R., Isaacman-VanWertz, G., Kreisberg, N. M., and Knote, C.: Effects of anthropogenic emissions on aerosol formation from isoprene and monoterpenes in the southeastern United States, Proceedings of the National Academy of Sciences, 112, 37-42, 2015.
Xue, J., Yuan, Z., Griffith, S. M., Yu, X., Lau, A. K. H., and Yu, J. Z.: Sulfate Formation Enhanced by a Cocktail of High NOx, SO_2, Particulate Matter, and Droplet pH during Haze-Fog Events in Megacities in China: An Observation-Based Modeling Investigation, Environ. Sci. Technol., 50, 7325-7334, 10.1021/acs.est.6b00768, 2016.
Yao, M., Zhao, Y., Hu, M. H., Huang, D. D., Wang, Y. C., Yu, J. Z., and Yan, N. Q.: Multiphase Reactions between Secondary Organic Aerosol and Sulfur Dioxide: Kinetics and Contributions to Sulfate Formation and Aerosol Aging, Environmental Science & Technology Letters, 6, 768-774, 10.1021/acs.estlett.9b00657, 2019.
Ye, C., Liu, P., Ma, Z., Xue, C., Zhang, C., Zhang, Y., Liu, J., Liu, C., Sun, X., and Mu, Y.: High H_2O_2 Concentrations Observed during Haze Periods during the Winter in Beijing: Importance of H_2O_2 Oxidation in Sulfate Formation, Environmental Science & Technology Letters, 5, 757-763, 10.1021/acs.estlett.8b00579, 2018.
Young, L.-H., Li, C.-H., Lin, M.-Y., Hwang, B.-F., Hsu, H.-T., Chen, Y.-C., Jung, C.-R., Chen, K.-C., Cheng, D.-H., and Wang, V.-S.: Field performance of a semi-continuous monitor for ambient $PM_{2.5}$ water-soluble inorganic ions and gases at a suburban site, Atmos. Environ., 144, 376-388, 2016.
Yu, H., Li, W., Zhang, Y., Tunved, P., Dall'Osto, M., Shen, X., Sun, J., Zhang, X., Zhang, J., and Shi, Z.: Organic coating on sulfate and soot particles during late summer in the Svalbard Archipelago, Atmos. Chem. Phys., 19, 10433-10446, 10.5194/acp-19-10433-2019, 2019.
Yue, F., He, P., Chi, X., Wang, L., Yu, X., Zhang, P., and Xie, Z.: Characteristics and major influencing factors of sulfate production via heterogeneous transition-metal-catalyzed oxidation during haze evolution in China, Atmos. Pollut. Res., 11, 1351-1358, https://doi.org/10.1016/j.apr.2020.05.014, 2020.
Zelenov, V. V., Aparina, E. V., Kashtanov, S. A., and Shardakova, E. V.: Kinetics of NO3 uptake on a methane soot coating, Russian Journal of Physical Chemistry B, 11, 180-188, 10.1134/s1990793117010146, 2017.
Zhang, B., Zhou, T., Liu, Y., Yan, C., Li, X., Yu, J., Wang, S., Liu, B., and Zheng, M.: Comparison of water-soluble inorganic ions and trace metals in $PM_{2.5}$ between online and offline measurements in Beijing during winter, Atmos. Pollut. Res., 10, 1755-1765, https://doi.org/10.1016/j.apr.2019.07.007, 2019.
Zhang, N., Zhang, J., Zhang, Y., Bai, J., and Wei, X.: Solubility and Henry's law constant of sulfur dioxide in aqueous polyethylene glycol 300 solution at different temperatures and pressures, Fluid Phase Equilibria, 348, 9-16, https://doi.org/10.1016/j.fluid.2013.03.006, 2013.
Zhang, X., Zhuang, G., Chen, J., Wang, Y., Wang, X., An, Z., and Zhang, P.: Heterogeneous Reactions of Sulfur Dioxide on Typical Mineral Particles, The Journal of Physical Chemistry B, 110, 12588-12596, 10.1021/jp0617773, 2006.
Zhao, D., Song, X., Zhu, T., Zhang, Z., Liu, Y., and Shang, J.: Multiphase oxidation of SO_2 by NO_2 on

$CaCO_3$ particles, Atmos. Chem. Phys., 18, 2481-2493, 10.5194/acp-18-2481-2018, 2018.
Zhao, S., Tian, H., Luo, L., Liu, H., Wu, B., Liu, S., Bai, X., Liu, W., Liu, X., Wu, Y., Lin, S., Guo, Z., Lv, Y., and Xue, Y.: Temporal variation characteristics and source apportionment of metal elements in PM2.5 in urban Beijing during 2018 – 2019, Environ. Pollut., 268, 115856, https://doi.org/10.1016/j.envpol.2020.115856, 2021.
Zheng, B., Zhang, Q., Zhang, Y., He, K. B., Wang, K., Zheng, G. J., Duan, F. K., Ma, Y. L., and Kimoto, T.: Heterogeneous chemistry: a mechanism missing in current models to explain secondary inorganic aerosol formation during the January 2013 haze episode in North China, Atmos. Chem. Phys., 15, 2031-2049, 10.5194/acp-15-2031-2015, 2015.
Zheng, H., Song, S., Sarwar, G., Gen, M., Wang, S., Ding, D., Chang, X., Zhang, S., Xing, J., Sun, Y., Ji, D., Chan, C. K., Gao, J., and McElroy, M. B.: Contribution of Particulate Nitrate Photolysis to Heterogeneous Sulfate Formation for Winter Haze in China, Environmental Science & Technology Letters, 7, 632-638, 10.1021/acs.estlett.0c00368, 2020.
Zhu, Y., Tilgner, A., Hoffmann, E. H., Herrmann, H., Kawamura, K., Yang, L., Xue, L., and Wang, W.: Multiphase MCM–CAPRAM modeling of the formation and processing of secondary aerosol constituents observed during the Mt. Tai summer campaign in 2014, Atmospheric Chemistry and Physics, 20, 6725-6747, 2020a.
Zhu, Y., Li, W., Lin, Q., Yuan, Q., Liu, L., Zhang, J., Zhang, Y., Shao, L., Niu, H., Yang, S., and Shi, Z.: Iron solubility in fine particles associated with secondary acidic aerosols in east China, Environ. Pollut., 264, 114769, https://doi.org/10.1016/j.envpol.2020.114769, 2020b.